On Stabilization of Cart-Inverted Pendulum System: An Experimental Study

T Rakesh Krishnan

Department of Electrical Engineering

National Institute of Technology

Rourkela-769008, India

July, 2012

On Stabilization of Cart-Inverted Pendulum System: An Experimental Study

A thesis submitted in partial fulfillment of the requirements

for the award of the award of degree

Master of Technology by Research

in

Electrical Engineering

by

T Rakesh Krishnan

Roll No: 610EE102

Under the guidance of

Prof. Bidyadhar Subudhi

Department of Electrical Engineering

National Institute of Technology

Rourkela-769008, India

2010-2012

Department of Electrical Engineering

National Institute of Technology, Rourkela

CERTIFICATE

*This is to certify that the thesis titled "**On Stabilization of Cart-Inverted Pendulum System: An Experimental Study**", by **Mr. T Rakesh Krishnan**, submitted to the National Institute of Technology. Rourkela (Deemed University) for the award of Master of Technology by Research in Electrical Engineering is a record of bona fide research work carried out by him in the Department of Electrical Engineering, under my supervision. We believe that this thesis fulfills part of the requirements for the award of degree of Master of Technology by Research. The results embodied in this thesis have not been submitted for the award of any degree elsewhere.*

_____

Place: Rourkela **Prof. Bidyadhar Subudhi**

Date:

Dedicated to

My Wonderful Amma and Appa

My beloved Teacher (Mrs. Indhu.P.Nair)

My Aunt (Ms. Bhagyalakshmi Venkatesh)

Acknowledgements

When the world says, "Give up,"
Hope whispers, "Try it one more time." - Author Unknown

The journey towards pursuing one's own dream is highly tormenting and demanding. The path it takes, the unexpected twists and turns that occurs, the element of hope is the only factor that inspires to live up to one's dream. Throughout my life a beacon of light has guided me from one hope to the other. I thank this light for its unconditional support.

The two long years during my M. Tech (Research) in Control and Robotics Lab has been highly satisfying. I have been blessed with the opportunity to work with great teachers Dr. Arun Ghosh, Prof. Bidyadhar Subudhi and Dr. Sandip Ghosh. Dr. Ghosh introduced me to this Inverted Pendulum control problem, and had to leave NIT Rourkela in a year. His vision and full support gave a base to this thesis.

Then, I came under the guidance of Prof. Subudhi. He has always been positive and in high spirits. He is a 'power house of knowledge'. He is really down to earth, and helps unconditionally throughout.

Dr. Sandip Ghosh has been very supporting and all encouraging. He is synonymous with simplicity. I would also use this opportunity to thank Dr. Chitti Babu who has been really a good friend to me and has encouraged me. I would take this opportunity to thank all the students of control and robotics lab- Dushmanta Sir, Shantanu Sir, Raseswari Madam, Raja Sir, Abhisek Behera, Koena di, Basant Sir, Satyam Sir, Srinibas Sir. All my classmates in control and automation, Madan, Susant, Om Prakash, Prawesh, Murali and many more.

I take this opportunity to thank my parents Mr. T. S. Krishnamoorthy and Mrs. Rema Krishnan, my brothers Ramesh and Achu, my mentor cum aunt Bhagyam attai. I would apologise if I have failed to acknowledge any body.

T Rakesh Krishnan

Abstract

The Cart-Inverted Pendulum System (CIPS) is a classical benchmark control problem. Its dynamics resembles with that of many real world systems of interest like missile launchers, pendubots, human walking and segways and many more. The control of this system is challenging as it is highly unstable, highly non-linear, non-minimum phase system and under-actuated. Further, the physical constraints on the track position control voltage etc. also pose complexity in its control design.

The thesis begins with the description of the CIPS together with hardware setup used for research, its dynamics in state space and transfer function models. In the past, a lot of research work has been directed to develop control strategies for CIPS. But, very little work has been done to validate the developed design through experiments. Also robustness margins of the developed methods have not been analysed. Thus, there lies an ample opportunity to develop controllers and study the cart-inverted pendulum controlled system in real-time.

The objective of this present work is to stabilize the unstable CIPS within the different physical constraints such as in track length and control voltage. Also, simultaneously ensure good robustness. A systematic iterative method for the state feedback design by choosing weighting matrices key to the Linear Quadratic Regulator (LQR) design is presented. But, this yields oscillations in cart position. The Two-Loop-PID controller yields good robustness, and superior cart responses. A sub-optimal LQR based state feedback subjected to H_∞ constraints through Linear Matrix Inequalities (LMIs) is solved and it is observed from the obtained results that a good stabilization result is achieved. Non-linear cart friction is identified using an exponential cart friction and is modeled as a plant matrix uncertainty. It has been observed that modeling the cart friction as above has led to improved cart response. Subsequently an integral sliding mode controller has been designed for the CIPS. From the obtained simulation and experiments it is seen that the ISM yields good robustness towards the output channel gain perturbations. The efficacies of the developed techniques are tested both in simulation and experimentation.

It has been also observed that the Two-Loop PID Controller yields overall satisfactory response in terms of superior cart position and robustness. In the event of sensor fault the ISM yields best performance out of all the techniques.

Contents

List of Abbreviations

Abbreviation	Description
CIPS	Cart-Inverted Pendulum System
SIMO	Single-Input-Multi-Output
IFAC	International Federation of Automatic Control
DC	Direct Current
LQR	Linear Quadratic Regulator
ITAE	Integral Time Absolute Error
LMI	Linear Matrix Inequality
SIRM	Single Input Rule Module
MARFC	Model Adaptive Reference Fuzzy Controller
GA	Genetic Algorithm
WNCS	Wireless Networked Control system
DMC	Dynamic Matrix Control
FLC	Fuzzy Logic Controller
SMC	Sliding Mode Control
ISM	Integral Sliding Mode
PID	Proportional Integral Derivative
YALMIP	Yet Another LMI Parser
DOF	Degrees Of Freedom
FBD	Free Body Diagram
ISR	Interrupt Service Routine

A/D	Analog-to-Digital
D/A	Digital-to-Analog
TLC	Target Language Compiler
PD	Proportional-Derivative
PI	Performance Index
CF	Cost Functional
ARE	Algebraic Riccati Equation
RMS	Root Mean Square
ISM	Integral Sliding Mode

List of Figures

List of Tables

Chapter 1

Introduction

The International Federation of Automatic Control (IFAC) Theory Committee in the year 1990 has determined a set of practical design problems that are helpful in comparing new and existing control methods and tools so that a meaningful comparison can be derived. The committee came up with a set of real world control problems that were included as “benchmark control problems”. Out of which the cascade inverted pendula control problem is featured as highly unstable, and the toughness increases with increase in the number of links.

The simplest case of this system is the cart- single inverted pendulum system. It also has very good practical applications right from missile launchers to segways, human walking, luggage carrying pendubots, earthquake resistant building design etc. The Inverted Pendulum dynamics resembles the missile or rocket launcher dynamics as its center of gravity is located behind the centre of drag causing aerodynamic instability.

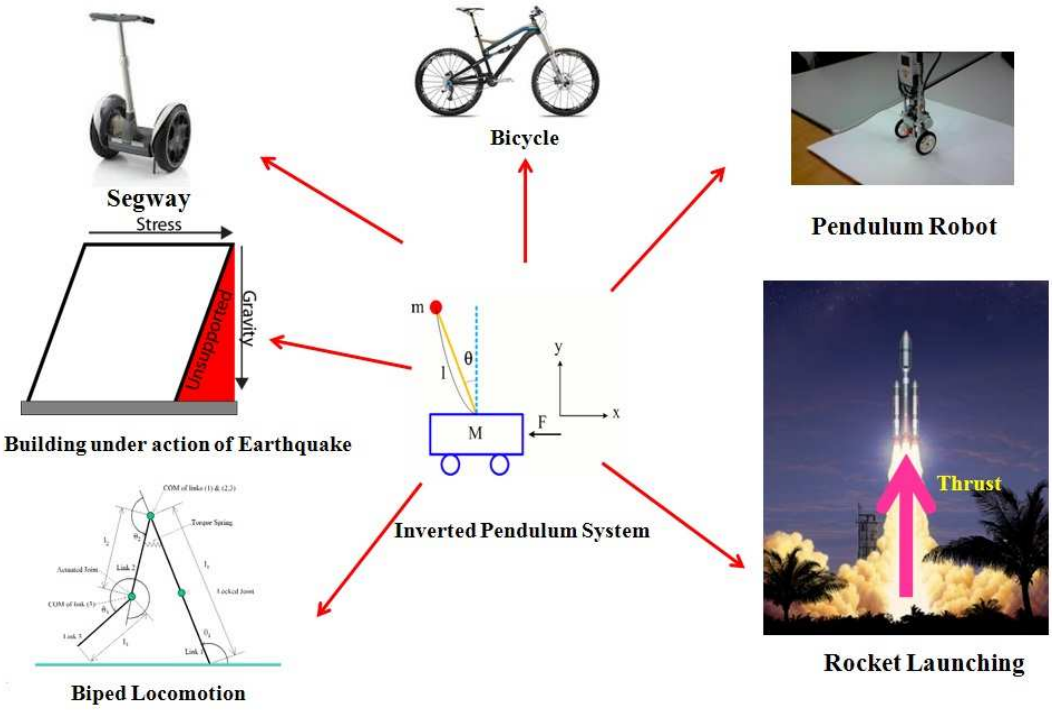

Fig.1.1.Inverted Pendulum like systems

1.1. Introduction to Inverted Pendulum Control Problem

The stabilization of inverted pendulum is a classical benchmark control problem. It is a simple system in terms of mechanical design only consisting of a D.C. Motor, a pendant type pendulum, a cart, and a driving mechanism. Fig.1.1.shows the basic schematic for the cart-inverted pendulum system

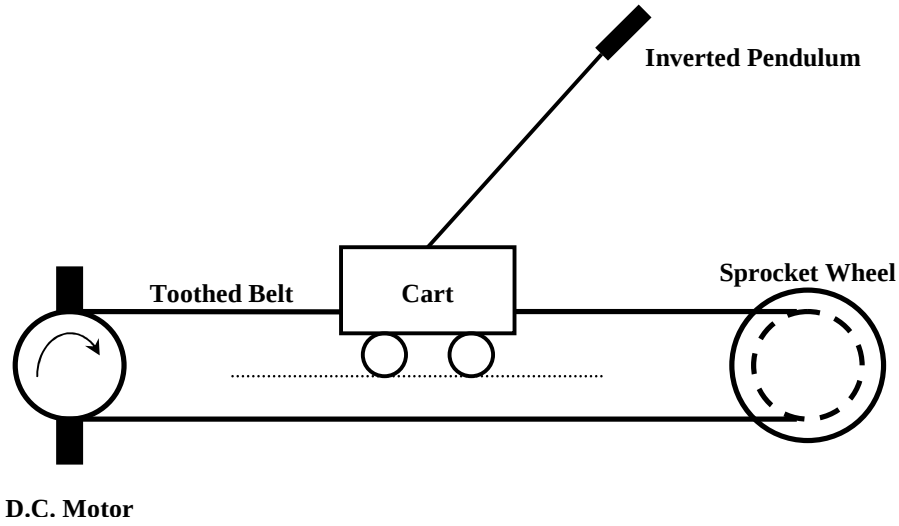

Fig.1.2.Inverted Pendulum system Schematic

The Inverted Pendulum is a single input multi output (SIMO) system with control voltage as input, cart position and pendulum angle as outputs. Even though the system is simple from construction point of view, but there lies a lot of control challenge owing to following characteristics .

- ***Highly Unstable*** – The inverted position is the point of unstable equilibrium as can be seen from the non-linear dynamic equations.
- ***Highly Non-linear*** – The dynamic equations of the CIPS consists of non-linear terms.
- ***Non-minimum phase system*** – The system transfer function of CIPS contains right hand plane zeros, which affect the stability margins including the robustness.
- ***Underactuated*** – The system has two degrees of freedom of motion but only one actuator i.e. the D.C. Motor. Thus, this system is under-actuated. This makes the system cost-effective but the control problem becomes challenging.

Additionally there are constraints imposed by track length, control voltage etc. These make the problem still more complex. This control problem attracts attention explains the various control approaches that is in attempt to stabilize the unstable system.

1.2. Inverted Pendulum Systems

1.2.1. Inverted Pendulum Dynamics

This section derives the dynamics of inverted pendulum dynamics from the Newton's laws of motion. The mechanical system has Two Degrees of freedom (DOF), the linear motion of the cart in the X-axis, the rotational motion of the pendulum in the X-Y plane. Thus there will be two dynamic equations.

Fig.1.3 shows the parametric representation of the Inverted Pendulum system. Let x be the distance in m from the Y-axis, and θ be the angle in rad w.r.t vertical.

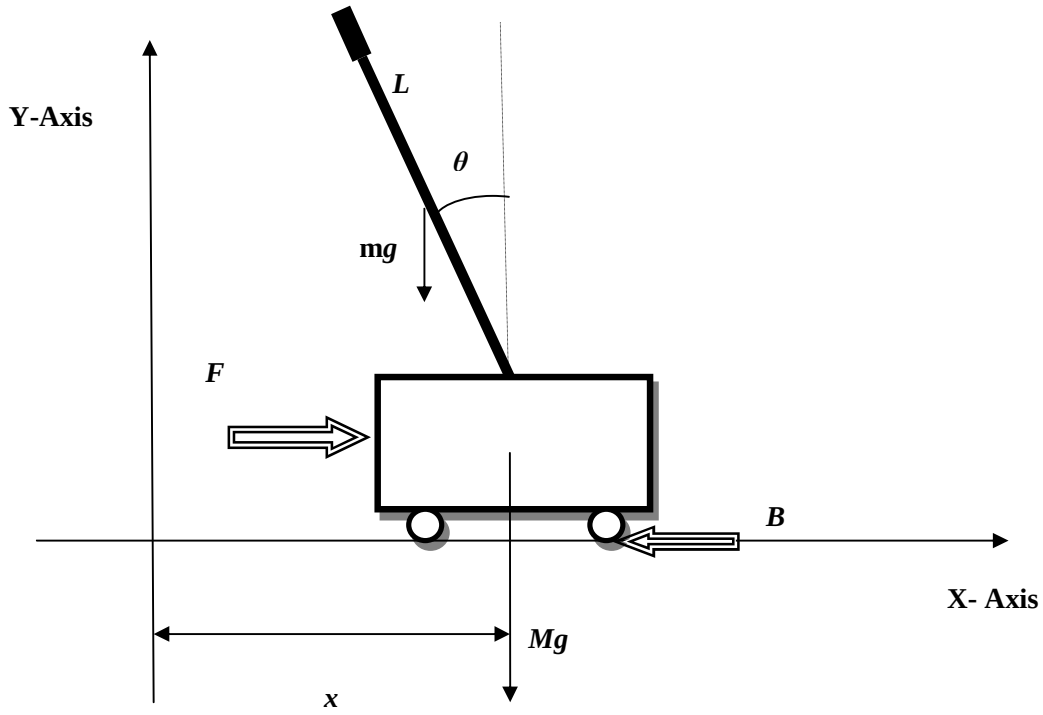

Fig.1.3. Parametric representation of the Inverted Pendulum System

Following is the list of parameters used in the derivation of Inverted Pendulum dynamics

M – Mass of cart in kg

m – Mass of Pendulum in kg

J – Moment of Inertia of pendulum in kg-m^2

L – Length of Pendulum in m

b – Cart friction coefficient in Ns/m

g – Acceleration due to gravity in m/s^2

Let us first analyze the free body diagram (FBD) of the cart as in Fig.1.4.

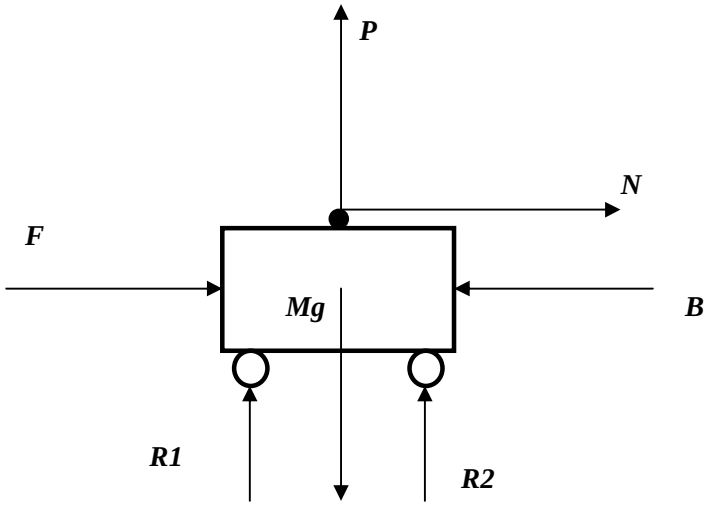

Fig.1.4. Free Body Diagram of the Cart

In Fig.1.4. only the horizontal forces are considered in the analysis as they only give information about the dynamics since the cart has only linear motion.

$$Ma_x = F + N - B \tag{1.1}$$

Here a_x is the acceleration in the horizontal direction.

The horizontal reaction N is given by the horizontal force due to the pendulum on the cart. This is given by

$$N = m\frac{d^2}{dt^2}(x + L\sin\theta) = m\ddot{x} + m\ddot{\theta}L\cos\theta - m(\dot{\theta})^2 L\sin\theta \tag{1.2}$$

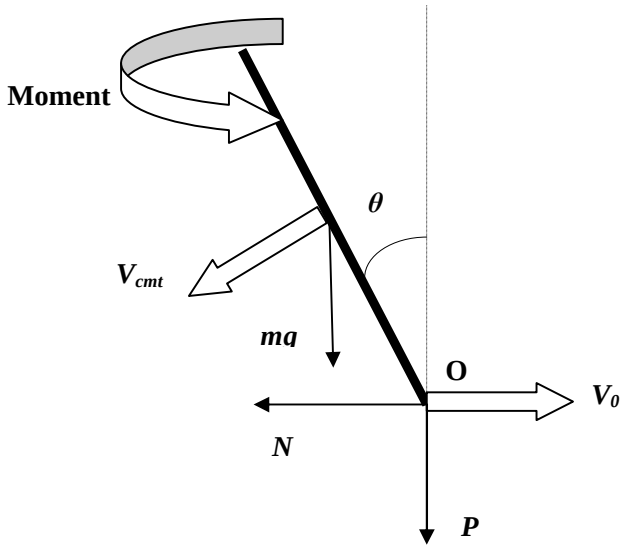

Fig.1.5. Free Body Diagram of Pendulum

Considering the FBD of the pendulum in Fig.1.5 the vertical reaction P is given by the weight of the pendulum on the cart. Let $L\cos\theta$ be the displacement of pendulum from the pivot. Then, P is given by

$$\begin{aligned} &P + mg = m\frac{d^2}{dt^2}(L\cos\theta) \\ &\Rightarrow P = mL\ddot{\theta}\sin\theta + mL(\dot{\theta})^2\cos\theta - mg \end{aligned} \tag{1.3}$$

In Fig.1.5.the moment due to the reaction forces P and N are resolved into X and Y directions. V_{cmt} is the velocity of centre of mass , V_o is the velocity of point O in the X direction. Summing the moments across the center we get

$$-NL\cos\theta - PL\sin\theta = J\ddot{\theta} \tag{1.4}$$

Substitution of (1.2) and (1.3) in (1.4) yields

$$mL\ddot{x}\cos\theta - (mL^2 + J)\ddot{\theta} = -mgL\sin\theta \tag{1.5}$$

After substituting (1.2) in (1.1) we get

$$\ddot{\theta} = \frac{mL}{\sigma}\left\{(F - b\dot{x})\cos\theta - mL(\dot{\theta})^2\cos\theta\sin\theta + (m+M)g\sin\theta\right\} \tag{1.6}$$

By solving (1.5) and (1.6) for $\ddot{x}$ we get after simplification

$$\ddot{x} = \frac{1}{\sigma}\left\{(J + mL^2)(F - b\dot{x} - mL\dot{\theta}^2\sin\theta) + mL^2 g\sin\theta\cos\theta\right\} \tag{1.7}$$

The parameter σ in (1.6) and (1.7) is given by

$$\sigma = mL^2(M + m\cos^2\theta) + J(M+m) \tag{1.8}$$

Equations (1.6) and (1.7) are the dynamic equations that describe the cart-pendulum system dynamics. Next section deals with the linear mathematical model for the inverted pendulum system

1.2.2. Linear Mathematical Model

A mathematical model can be defined as a set of mathematical equations that purports to represent some phenomenon in a way that gives insight into the origins and the consequences of the behavior of the system [4]. It is a well known fact that more accurate the model more complex the equations will be. It is always desirable to have a simple model as it is easy to understand. So we need to strike a balance between accuracy and simplicity.

It can be seen that the equations (1.6) to (1.8) are non-linear. In order to obtain a linear model the Taylor series expansion can be used to convert the non-linear equations to linear ones; finally give a linear model that will be helpful in linear control design.

Please note that the system has two equilibrium points one is the stable i.e. the pendant position and the other one is the unstable equilibrium point i.e. the inverted position. For our purpose we need to consider the second one as we require the linear model about this point. So, we assume a very small deviation θ from the vertical.

$$\begin{aligned}\theta &\approx 0\\ \sin\theta &= \theta\\ \cos\theta &= 1\\ \dot{\theta}^2 &= 0\end{aligned} \tag{1.9}$$

Linearizing (1.6) to (1.8) using (1.9)

$$\ddot{\theta} = \frac{mL}{\sigma'}\left\{\left(F - b\dot{x}\right) + \left(M+m\right)g\theta\right\} \tag{1.10}$$

$$\ddot{x} = \frac{1}{\sigma'}\left\{\left(J+mL^2\right)\left(F-b\dot{x}\right) + m^2L^2g\theta\right\} \tag{1.11}$$

Here $\sigma' = MmL^2 + J\left(M+m\right)$.

Inorder to obtain the state model we are assuming the states to be as the cart position x, cart linear velocity $\dot{x}$, pendulum angle θ, pendulum angular velocity $\dot{\theta}$. The state space is of the form

$$\dot{X} = AX + Bu \tag{1.12}$$

The state space for the Inverted Pendulum system is obtained as [1]

$$\begin{bmatrix}\dot{x}\\ \ddot{x}\\ \dot{\theta}\\ \ddot{\theta}\end{bmatrix} = \begin{bmatrix}0 & 1 & 0 & 0\\ 0 & -\dfrac{\left(J+mL^2\right)b}{\sigma'} & \dfrac{m^2L^2g}{\sigma'} & 0\\ 0 & 0 & 0 & 1\\ 0 & \dfrac{-\left(mLb\right)}{\sigma'} & \dfrac{mgL\left(M+m\right)}{\sigma'} & 0\end{bmatrix}\begin{bmatrix}x\\ \dot{x}\\ \theta\\ \dot{\theta}\end{bmatrix} + \begin{bmatrix}0\\ \dfrac{\left(J+mL^2\right)}{\sigma'}\\ 0\\ \dfrac{mL}{\sigma'}\end{bmatrix}F \tag{1.13}$$

The output equation is given by

$$y = \begin{bmatrix}1 & 0 & 0 & 0\\ 0 & 0 & 1 & 0\end{bmatrix}\begin{bmatrix}x\\ \dot{x}\\ \theta\\ \dot{\theta}\end{bmatrix} \tag{1.14}$$

We neglect the cart friction coefficient and thus we obtain a simplified transfer function in (1.15) and (1.16). The transfer function is given from state space

$$\frac{X(s)}{U(s)} = \frac{K_{actuator}\left\{\left(J + mL^2\right)s^2 - mgL\right\}}{s^2\left(\left(J\left(m+M\right) + MmL^2\right)s^2 - mgL\left(M+m\right)\right)} \tag{1.15}$$

$$\frac{\theta(s)}{U(s)} = \frac{K_{actuator}\left\{mLs^2\right\}}{s^2\left(\left(J\left(m+M\right) + MmL^2\right)s^2 - mgL\left(M+m\right)\right)} \tag{1.16}$$

The actuator gain $K_{actuator}$ is assumed to be a simple gain that converts voltage to force.

The following is the parameter table that gives the value of the various parameters that has been adopted from the Feedback Digital Pendulum Manual [3].

Table.1.1.Inverted Pendulum System Parameters[3]

Parameter	Value
Mass of Cart, M	**2.4 kg**
Mass of Pendulum, m	**0.23 kg**
Moment of Inertia of Pendulum, J	**0.099kg-m^2**
Length of Pendulum, L	**0.4 m**
Cart Friction Coefficient, b	**0.05 Ns/m**
Acceleration due to gravity, g	**9.81 m/s^2**
Actuator Gain , K$_{actuator}$	**15**

After substitution of parameters from Table 1.1 the state model and the transfer function model is obtained as

$$\begin{bmatrix} \dot{x} \\ \ddot{x} \\ \dot{\theta} \\ \ddot{\theta} \end{bmatrix} = \begin{bmatrix} 0 & 1 & 0 & 0 \\ 0 & 0 & 0.238 & 0 \\ 0 & 0 & 0 & 1 \\ 0 & 0 & 6.807 & 0 \end{bmatrix} \begin{bmatrix} x \\ \dot{x} \\ \theta \\ \dot{\theta} \end{bmatrix} + \begin{bmatrix} 0 \\ 5.841 \\ 0 \\ 3.957 \end{bmatrix} u \tag{1.17}$$

The transfer functions in (1.15) and (1.16) are substituted by the values in Table.1.1 we obtain

$$\frac{X(s)}{U(s)} = \frac{5.841(s^2 - 6.8068)}{s^2(s^2 - 6.807)} \approx \frac{5.841}{s^2} \tag{1.18}$$

$$\frac{\theta(s)}{U(s)} = \frac{3.957s^2}{s^2(s^2 - 6.807)} \approx \frac{3.957}{(s^2 - 6.807)} \tag{1.19}$$

Due to the approximate cancellation of the modes in both the transfer functions it is seen that both the feedbacks are necessary for all modes to be available for control. Next section explains the construction and working of the experimental setup.

1.2.3. Experimental Setup

The setup consists of the following are the requirements [2]

1. PC with PCI-1711 card
2. Feedback SCSI Cable Adaptor
3. Digital Pendulum Controller
4. DC Motor (Actuator)
5. Cart
6. Pendant Pendulum with weight
7. Optical encoders with HCTL2016 ICs
8. Track of 1m length with limit switches.
9. Adjustable feet with belt tension adjustment.
10. Software: MATLAB, SIMULINK, Real-Time Workshop, ADVANTECH PCI-1711 device driver, Feedback Pendulum Software.
11. Connection cables and wires.

The heart of the experimental setup is a cart and a pendant pendulum. The cart has four wheels to slide on the track. There are two coupled pendant pendulums; they have a pendant or bob that would make the pendulum more unstable that is because it shifts the centre of gravity to a higher level to the reference. The cart on the rail and is driven by a toothed belt which is driven by DC Motor. The motor drives the cart in a velocity proportional to the applied control voltage.

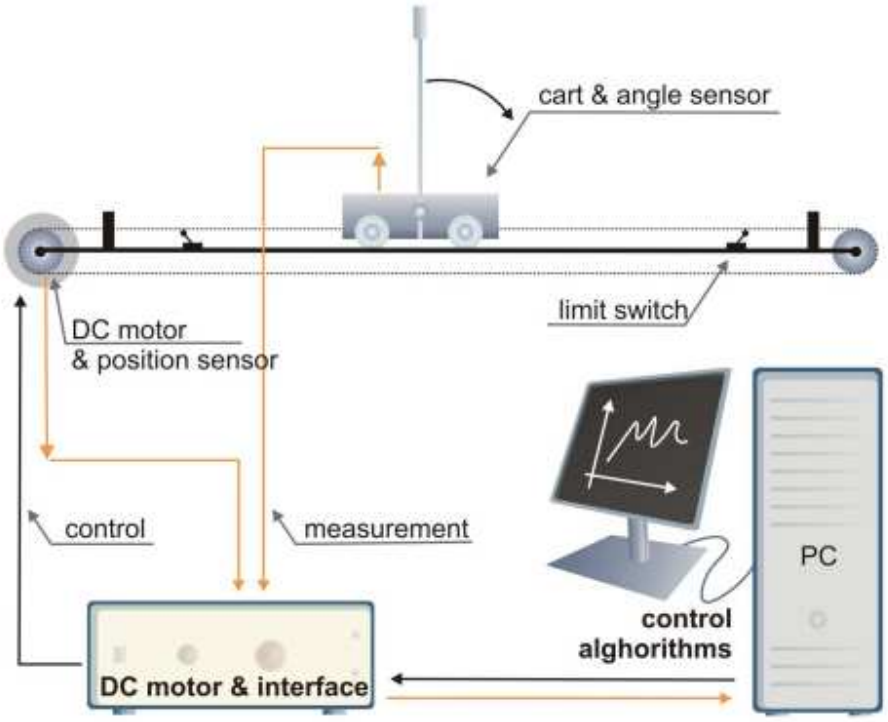

Fig.1.6.Feedback's Digital Pendulum Experimental Setup Schematic [3]

The motion of the cart is bounded mechanically and additionally for safety is improved by limit switches that cuts off power when the cart crosses them. Fig.1.7.shows the cutaway diagram showing the mounting of the sensors. The optical encoders have a light source and light detector and in between there is a rotating disc. Optical encoders are widely used in robotics, manufacturing, medical industry etc. A digital encoders outputs a pair of digital square signals 90^{o} apart i.e. quadrature to one another which convey the shaft's position change, as well as the direction of rotation. The rotational speed of the shaft can be determined from the encoder output. Longer is the period of the digital wave, slower the encoder turning. The resolution of the encoder is determined by the slit density of encoder wheel counts per revolution.

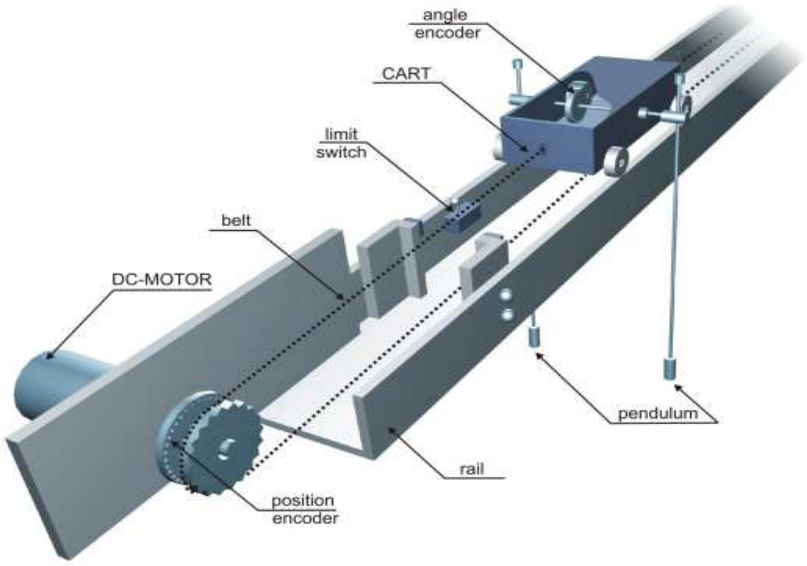

Fig.1.7.Cutaway Diagram Showing sensors and their mounting [2]

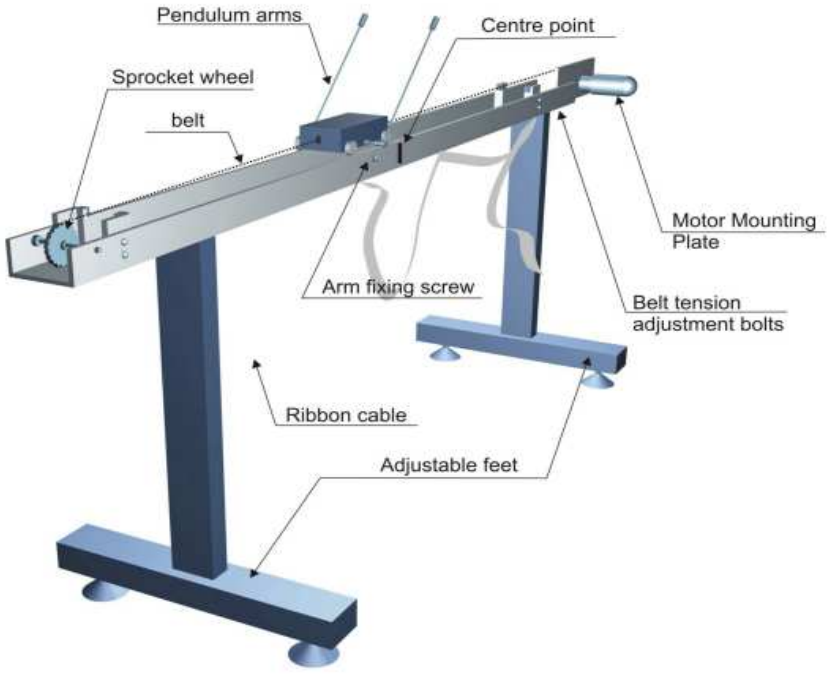

Fig.1.8.Digital Pendulum Mechanical Setup [2]

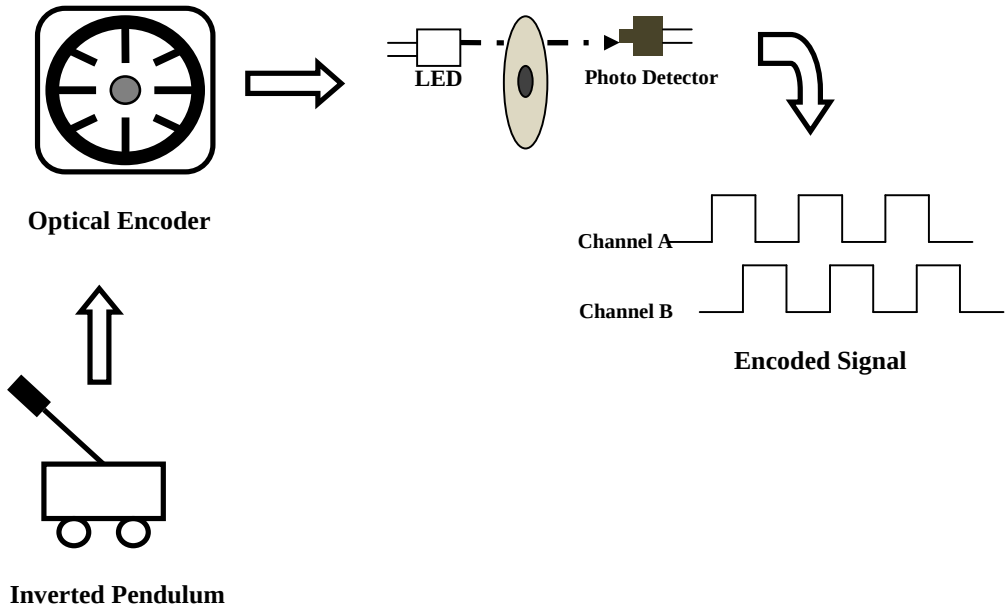

Fig.1.9.Optical Encoder operating principle

Fig 1.9. shows the operating principle of an optical encoder. The real time implementation of controller does not require building a new real time system. Already there exists a framework the can be edited as required. The required controller can be designed in SIMULINK and suitably tested in experiment through the Real-Time Workshop and control an external process through the PCI card.

The control algorithm and the A/D and D/A converters operate according to time pulses generated by the clock. The time between two consecutive pulses is called the sampling time.The clock delivers an interrupt and the Interrupt Service Routine (ISR). It is during this ISR that A/D delivers the discrete representation of the sensor measurement and based on this control algorithm calculates the required control value. At the end of the ISR the value is set in the D/A until the next sampling interval.

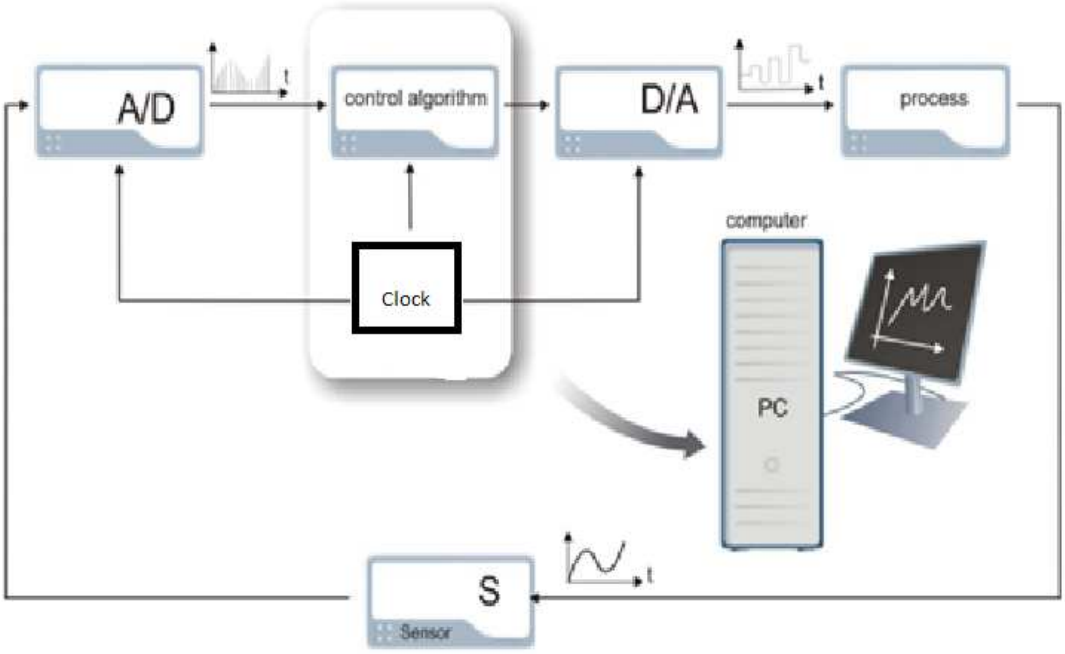

Fig.1.10.Computer based Control Algorithm [3]

The next section tries to explain how the SIMULINK and the Real-Time Workshop seamlessly integrate with the hardware.

1.2.4. Real-Time Workshop

The Real-Time Workshop is an extension of SIMULINK that has rapid prototyping ability for real-time software applications [5]. It has the following features

- Automatic code generation tailored for various target platforms.
- A rapid and direct path from system design to implementation.
- Seamless integration with MATLAB and SIMULINK.
- A simple graphical user interface.
- An open architecture and extensible make process.

The toolbox has an automatic program building process for real-time processes. Fig.1.11 explains the process diagrammatically. A high level m-file controls this build process.

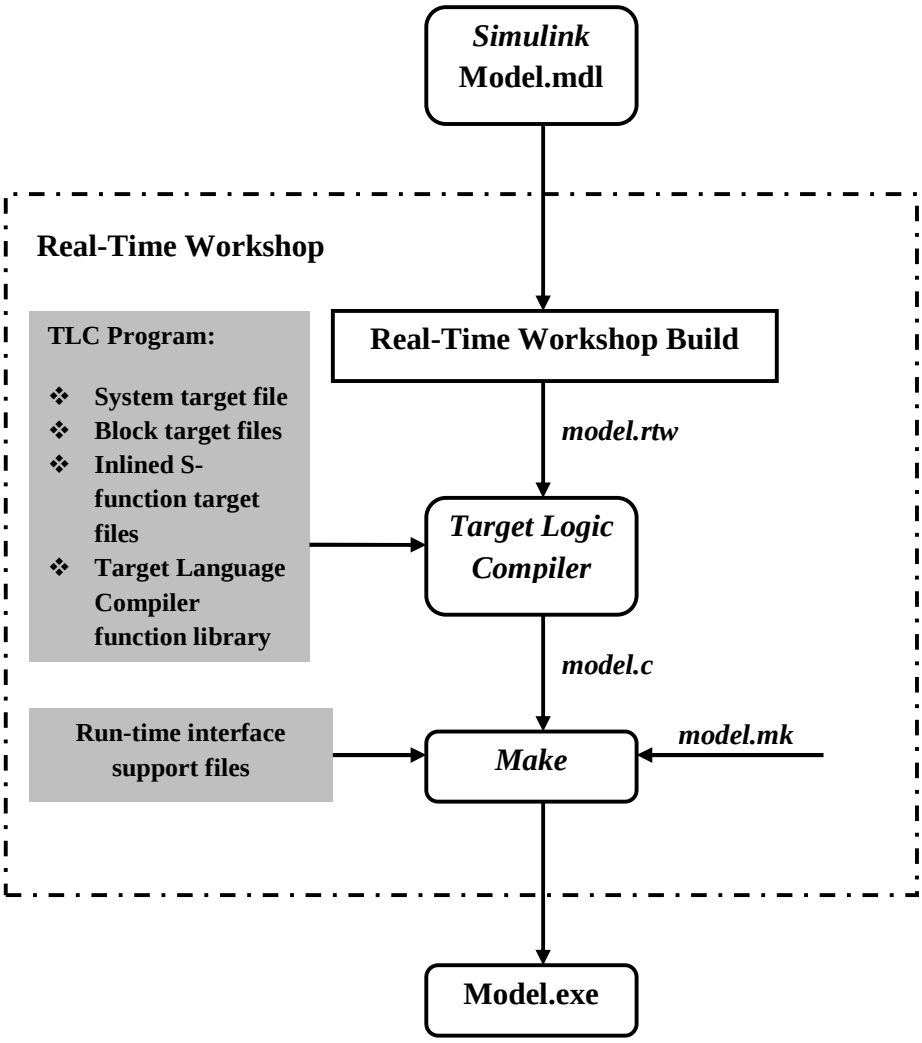

Fig.1.11.Real-Time Workshop working schematic [5]

Following are the steps in the real time build process [5]

1. Real-Time Workshop analyses the block diagram and compiles it into an intermediate hierarchical representation of the form ***model.rtw***.
2. The Target Language Compiler (TLC) reads the ***model.rtw*** and converts it into C code that is placed in the build directory within the MATLAB working directory.
3. The TLC constructs a makefile from an appropriate target makefile template and places in the build directory.

4. The system make utility reads the makefile to compile the source code and links object files and libraries and generate an executable file ***model.exe***.

This simple executable file is easily understood by hardware as it is in binary. Thus the control algorithm in high level language is seamlessly converted into an executable program by the toolbox. The next section introduces the practical problems that need to be addressed while designing any controller to inverted pendulum systems.

1.2.5. Physical Constraints on Inverted Pendulum Experimental Setup

The real inverted pendulum is a highly non-linear system as is evident from the derived mathematical model. Inorder, to reduce the model complexity it is advisable to linearize the model. But, this produces an additional constraint on the Region of Attraction of the initial Pendulum angle value due to model linearization. The track is of limited length of 1m, with limit switches placed at 0.1m from either edge. So any controller must stabilize the system within this length otherwise the limit switches trip making the system unstable.

It is well known that, practically motors have a voltage range and torque limit, there is a limit of ± 2.5 V. So to ensure safety we have used a saturation block that will limit this range. There should be also trade-off between the choice of damping between the position and angle. In literature there is sufficient evidence that the PD control in Inverted Pendulum leads to friction induced limit cycles (stick-slip friction) [6], [7].

1.3. Literature Review: Control Strategies applied to Cart-Inverted Pendulum system

The inverted pendulum since is an important control problem which the researchers have been trying to solve worldwide for last few decades. Historically, the Inverted Pendulum was used first by seismologists in design of a “seismometer” in the year 1844 in Great Britain. Since, the system is inherently in unstable equilibrium when mounted on a stiff wire it can sense even the slightest of vibrations.

Linear Quadratic Regulator (LQR) for inverted pendulum is simplest of all linear control techniques. It is equivalent to a two loop PD control design. In [8], stabilization of the cart-

pendulum system was carried out by linearization of the state model and designing a LQR after swing-up by an energy based controller. The velocity states were less penalized compared to the position states in [6] so that the resulting stabilized system will have almost zero position as a zero velocity is only a secondary priority. This logic will lead to an almost upright system.

There are two sets of poles one set is fast and other set is slow, the fast set of poles determine the angle dynamics and the slow set of poles determines the position dynamics. The cart position error always overshoots initially to catch up with the falling pendulum. Only after the rod is stabilized the position comes back to origin [9]. The effect of Inverted Pendulum under the linear state feedback has been analyzed in [10], the dynamic equations indicate the existence of stability regions in four dimensional state-space and an algorithm has been developed that transforms the four dimensional state space to three dimensional space. In [11], a tutorial has been presented wherein, the concept of digital control system design by pole placement with and without state estimation has been introduced.

A dynamic H_∞ compensation has been designed in [12] by considering dry friction and implemented in the Inverted Pendulum system. In [13], the authors have designed a robust periodic controller with zero placement capability for an Inverted Pendulum system.

A comparison of performances various controllers like PD, Siding Mode, Fuzzy, Expert Systems and Neural Network has been attempted in [14]. The comparison between various energy based swing up methods that swing the pendant pendulum to inverted pendulum has been attempted in [15], a special emphasis on the robustness of minimum time solutions is also presented. Various non-linear control methods have also been developed for the inverted pendulum stabilization problem. An Energy-speed-gradient method based Variable Structure controller has been designed and analyzed in [16] with global attractivity is guaranteed. A smooth feedback control law has been presented for almost global stabilization of inverted pendulum is given in [17], ensures asymptotic stability too. A Continuous time Sliding mode Control and Discrete Time Sliding mode controller has designed for an Inverted Pendulum system applied to an experimental setup with the help of a computer [18]. A method of Controlled Lagrangian has been developed for symmetrical systems; method of kinetic shaping is used to derive the control law and has been applied to inverted pendulum in [19]. A combined controller for both swing up and stabilization has been attempted in [20] using input-output linearization, energy control and

singular perturbation theory. A hybrid controller is designed in [21] that ensures global stabilization, this approach has a linear controller for stabilization, a linear cart controller and a combination of various bang-bang controllers for swing-up in minimum time. A non-linear controller is described in [22], in which the controller swings up the pendulum from the pendant position and stabilizes the pendulum in the unstable equilibrium and simultaneously restricts the cart excursion on the track. A simple controller for balancing the inverted pendulum to the upper equilibrium point and minimize the cart position to zero is discussed in [23]. A near optimal controller, non-linear control law has been designed based on linear quadratic optimal control yielding a near optimal gain schedule.

An implementation of intermittent linear-quadratic predictive pole-placement control is experimentally shown in [25] to achieve good performance when controlling a prestabilised inverted pendulum. A fuzzy based adaptive sliding mode controller is designed in [26], this controller automatically compensates for the plant non-linearity and tracks the cart-inverted pendulum system. An indirect adaptive Lyapunov based fuzzy controller is described in [27], the design is verified for the cart-inverted pendulum in simulation.

A self organizing fuzzy controller is designed in [28], and it is verified for an inverted pendulum system. Stability analysis for a Fuzzy model based nonlinear control using genetic algorithm with arithmetic crossover and non-uniform mutation, based on Lyapunov's stability theorem with a smaller number of Lyapunov conditions is given in [29] applied to inverted pendulum. Using exhaustive simulations a multi-local linear based Tagaki-Sugeno type in [30], this derived controller is found to ensure global stabilization and ensures stability of inverted pendulum in zero gravity condition in [31]. In this a two controller has been suggested there is a fuzzy swing-up controller for swing up, sliding two position controllers.

The choice of scaling factors in the design of fuzzy logic controllers as the performance of fuzzy logic based PID controllers greatly depended on these. The paper presents various methods for estimating scaling parameters for inverted pendulum using artificial intelligence in [32], based on ITAE criterion. Actuator saturation is of prime importance in design of control system design applied to experimental inverted pendulum system, this has been addressed with the help of Tagaki- Sugeno type Fuzzy logic based gain scheduling algorithm in [33], the modeling uncertainty is considered as a norm bounded uncertainty, the problem of defining the region of

attraction for T-S fuzzy systems based on normal state feedback is defined with the help of Linear Matrix Inequalities (LMIs). A new fuzzy logic controller based on Single Input Rule Modules (SIRMs) dynamically connected inference modules in [34]. The SIRMs are dynamically switched between the two modules one for angular position and the other for cart position, the controller switching takes place with a higher priority towards angular position.

A Model Adaptive Reference Fuzzy Controller (MARFC) in [35] wherein the fuzzy knowledge base is modified according to the error generated from the reference model and the actual plant. The stability of such a system is ensured in Lyapunov analysis, in simulation it has been shown that in case of zero disturbances the states converge to the origin but in the case of continuous excitation it is asymptotically stable.

It is difficult always to depict the control structure of a learning control system so in [36] the authors have attempted a three-phased framework for a learning based dynamic control system. The control law parameters are derived using Genetic Algorithm using lookup tables. An inverted pendulum is used to verify the reliability and robustness of the method. A self generating fuzzy logic controller is designed with the help of Genetic Algorithm (GA) in [37]. Each parameter of the fuzzy logic controller is tuned with the help of a fitness function to guide the searching algorithm.

An interesting work using extended Kalman Filter in [38] for sensor failure detection and identification, the algorithm is used to estimate the fault related parameter. A realistic evaluation of this algorithm is carried out on an inverted pendulum system. The failure test is authenticated by applying various types of failures. An experimental work is carried out in order to study the effect of delay on a Wireless Networked Control system (WNCS) with application to a cart-inverted pendulum setup in [39], a new Gaussian model for delay analysis is used together with Dynamic Matrix Control (DMC) and LQ control together with multiple observers. The advantages and drawbacks of using a vision based feedback is demonstrated with the help of a fuzzy logic based Inverted pendulum control in [40]. A Fuzzy Logic Controller (FLC) is used in [41] to combine an Sliding Mode Control (SMC) based swing up controller and a State Feedback based stabilization controller and the advantages attained by this control is also demonstrated.

An algorithm is defined to handle time delays in a feedback control loop in which both the control loops with different measurement signals through variable time delays and packet loss in [42], an algorithm is developed to estimate random time delay and its effects are illustrated on an inverted pendulum setup . The presence of transient overload can cause unpredictable behavior in computer control systems, this problem is usually increasing the activation period intervals in which the control law is updated this will cost the control performance. In [43] a new elastic scheduling method has been proposed in which the overload is completely eliminated and effectiveness is demonstrated in a real inverted pendulum set up.

1.4. Objectives of the Thesis

- To stabilize the unstable cart-pendulum system simultaneously meeting the physical constraints imposed.
- To identify the non-linear cart friction that will be helpful in reducing the modeling error and will decrease the stick-slip oscillations (friction memory).
- To develop various stabilizing controllers like Linear Quadratic Regulator (LQR), Two-Loop-PID, State feedback design by sub-optimal LQR subjected to H_∞ constraints and Integral Sliding Mode (ISM) design by pole placement.
- The robustness of all these compensated schemes have also be analysed in respective chapters.

1.5. Organisation of the Thesis

The thesis contains six chapters as follows

- **Chapter 1** – Introduces the classical Inverted Pendulum Control problem, its dynamics, its mathematical model both in state space and transfer function. It also describes the experimental setup. It also describes the integration between the hardware (experimental setup), MATLAB, SIMULINK, REALTIME WORKSHOP. The chapter describes the basic problems faced in its implementation.
- **Chapter 2**- Describes the Linear Quadratic Regulator based state feedback control law design. It describes the logic used in weight selection of the weighted matrices key to the LQR design. The chapter ends with the simulation and experimental results obtained, and a robustness analysis is also presented in the end.

- **Chapter 3** – This chapter deals with the design of two loop PID controller using pole placement. The key to the design is the derivation of the pole placement equation. The chapter concludes with the responses obtained in both simulation and through experiment together with the robustness verification at the end.
- **Chapter 4** – The chapter begins with the explanation of concepts behind feedback, robustness, various sensitivity functions, concept of H_∞ in control design. It then goes on to derive the Linear Matrix Inequalities (LMIs) for sub-optimal LQR, H_∞ based state feedback, maximum control signal magnitude. Then combines and then solves these objectives together for the inverted pendulum control problem using the YALMIP toolbox. The chapter ends with the results obtained in simulation and real-time and also demonstrates the result of various robustness tests.
- **Chapter 5** –The chapter then goes on to explain the concept of Integral sliding mode and its design by pole placement. A complete section is devoted towards on how the effect of dynamic friction is modeled as a plant matrix uncertainty. The design starts with the derivation of control law, then the law is applied to the inverted pendulum stabilization problem and the result and analysis are shown.
- **Chapter 6** – Draws conclusions on the various works presented and aptly suggests the scope of future work.

Chapter 2

Linear Quadratic Regulator (LQR) design applied to cart-inverted pendulum system

LQR algorithm in comparison with conventional pole placement method automatically chooses closed loop according to the weights which in turn depend on system constraints. The chapter presents a brief description of the LQR concept. The points to be kept in mind before designing an LQR based state feedback are also given. Since, the choice of the LQR is the key towards LQR design, a systematic weight selection for the CIPS is presented. The detailed analysis of the simulation and experimental results is presented.

2.1. Linear Quadratic Regulator

The LQR is one of the most widely used static state feedback methods, primarily as the LQR based pole placement helps us to translate the performance constraints into various weights in the performance index. This flexibility is the sole reason for its popularity. As seen in Chapter 1 the cart-inverted pendulum system has many physical constraints both in the states and in the control input. Hence, the LQR design is attempted. The choice of the quadratic performance indices depends on physical constraints and desired closed loop performance of the control system. Any state feedback can be generalized for an LTI system as given below:

$$\begin{aligned} \dot{x} &= Ax + Bu \\ y &= Cx \end{aligned} \tag{2.1}$$

If all the n states are available for feedback and the states are completely controllable then there is a feedback gain matrix K, such that the state feedback control input is given by

$$u = -K(x - x_d) \tag{2.2}$$

Let x_d be the vector of desired states. The closed loop dynamics using (2.2) in (2.1) becomes

$$\dot{x} = (A - BK)x + BKx_d \tag{2.3}$$

Choice of *K* depends on the desired pole locations where one intends to place the poles such that the desired control performance be achieved. In the case of LQR the control is subjected to a Performance Index (PI) or Cost Functional (CF) given by

$$J = \frac{1}{2}[z(t_f) - y(t_f)]^T F(t_f)[z(t_f) - y(t_f)] + \frac{1}{2}\int_{t_o}^{t_f} \left\{[z-y]^T Q[z-y] + u^T Ru\right\} dt \tag{2.4}$$

Here *z* is the *m* dimensional reference vector and *u* is an *r* dimensional input vector. If all the states are available in the output for feedback then *m* becomes *n*. Since, the performance index (2.4) is in terms of quadratic terms of error and control it is called as quadratic cost functional. If our objective is to keep the system state to near zero then it is called as a state regulator system. Here the unwanted plant disturbances that need to be rejected e.g. Electrical Voltage Regulator System. If it is desire to keep the output or state near a desired state or output it is called a tracking system as for example an antenna control system where tracking of an aircraft is the requirement.

In (2.4), the matrix *Q* is known as the error weighted matrix, *R* is the control weighted matrix, *F* is known as the terminal cost weighted matrix. The following points may be noted for the LQR implementation

- All the weighted matrices are symmetric in nature.
- The error weighted matrix *Q* is positive semi-definite as to keep the error squared positive. Due to quadratic nature of PI, more attention is being paid for large errors than small ones. Usually it is chosen as a diagonal matrix.
- The control weighted matrix *R* is always positive definite as the cost to pay for control is always positive. One has to pay more cost for more control.
- The terminal cost weighted $F(t_f)$ is to ensure that the error e(t) reaches a small value in a finite time t_f .So the matrix should always be positive semi-definite.

Usually an Infinite Time LQR problem is of more interest where the final end cost $F(t_f)$ is zero. In this case the PI in (2.4) becomes

$$J = \int_{t_o}^{\infty} \frac{1}{2}\{x'Qx + u'Ru\}\,dt \tag{2.5}$$

By applying Pontryagin's Maximum Principle on the open loop system an optimal solution for the closed loop system we is obtained following equations are resulted

$$\begin{aligned} &\dot{x} = Ax + Bu,\ x(t_o) = x_o \\ &\dot{\lambda} = -Qx - A^T\lambda, \lambda(t_f) = 0 \\ &Ru + B^T\lambda = 0 \end{aligned} \tag{2.6}$$

Since all the equations in (2.6) are linear these can be connected by

$$\lambda = Px \tag{2.7}$$

By substituting for $\dot{\lambda}$ from (2.6) and then substituting for $\dot{x}$ from (2.6) and using (2.7) by substituting for u from (2.6) we get

$$PAx + A^T Px + Qx - PBR^{-1}B^T Px + \dot{P} = 0 \tag{2.8}$$

This is called Matrix Riccati Equation. The steady state solution is given by

$$PA + A^T P + Q - PBR^{-1}B^T P = 0 \tag{2.9}$$

The above equation is called Algebraic Riccati Equation (ARE). The optimal state feedback is obtained from $Ru + B^T\lambda = 0$ as

$$\begin{aligned} u &= -R^{-1}B^T Px \\ &= -Kx \end{aligned} \tag{2.10}$$

The static gain vector K is called Kalman gain.

2.1.1. Features of LQR

- As the feedback is static the closed loop system order is the system is same as the open loop plant.
- The LQR ensures infinite gain margin and phase margin greater than or equal to 60^o on the output side [45], [58], [59].

- In the case when we want to minimize output the weighting matrix Q becomes $Q = C^T Q' C$ where Q' is the auxillary weighting matrix.

2.2. LQR Control Design

The choice of Q and R is very important as the whole LQR state feedback solution depends on their choice. Usually they are chosen as identity values and are successively iterated to obtain the controller parameter. In [44] *Bryson's Rule* is also available for constrained system, the essence of the rule is just to scale all the variables such that the maximum value of each variable is one . *R* is chosen as a scalar as the system is a single input system.

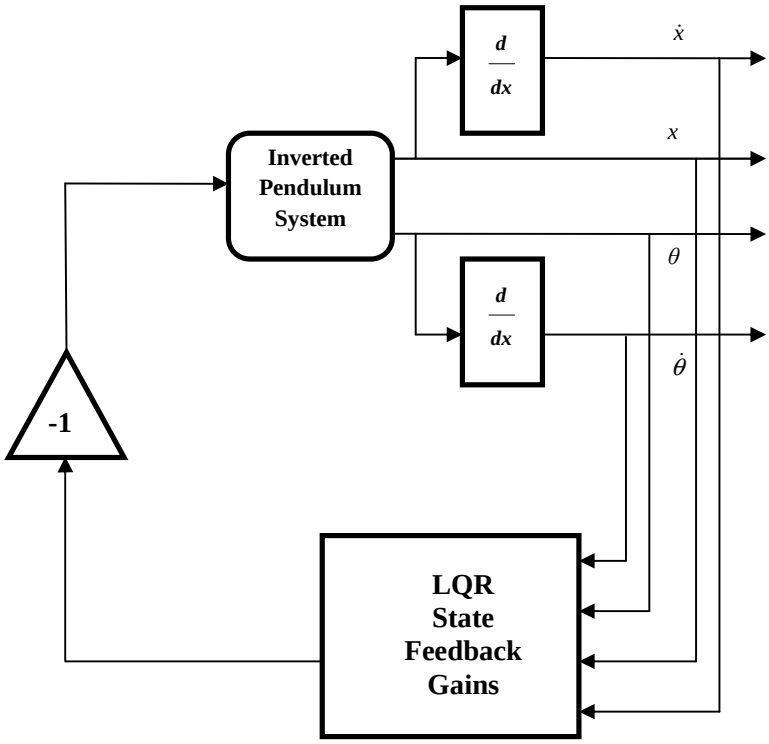

Fig.2.1.Linear Quadratic Regulator applied to Inverted Pendulum System

The excitation due to initial condition is reflected in the states can be treated as an undesirable deviation from equilibrium position. If the system described by (2.1) is controllable then it is possible to drive the system into its equilibrium point. But it is very difficult to keep the control

signal within bound as chances are such that the control signal would be very high which will lead to actuator saturation and would require high bandwidth designs in feedback that might excite the unmodelled dynamics [45]. Hence, it required to have a trade-off between the need for regulation and the size of the control signal. It can be seen that the choice of control weighting matrix *R* comes handy in keeping the control signal magnitude small. It can be seen that larger the weight on *R* the smaller is the value of the control signal.

The logic behind choice of weights of *Q* (usually chosen as a diagonal matrix) is relative that the state that requires more control effort requires more weightage than the state that requires less control. It may be useful to note the limitations of LQR design [45]:

- Full state feedback requires all the states to be available; this limits the use of LQR in flexible structures as such systems would infinite number of sensors for complete state feedback.
- The LQR is an optimal control problem subjected to certain constraints so the resultant controller usually do not ensure disturbance rejection as it indirectly minimizes the sensitivity function, reduction in overshoot during tracking, stability margins on the output side etc.
- Optimality does not ensure performance always.
- LQR design is entirely an iterative process that as the LQR doesn't ensure standard control system specifications, even though it provides optimal and stabilizing controllers. Hence, several trial and error attempts is required to ensure satisfactory control design.

The following is the algorithm that has been used in the LQR control design for cart-inverted pendulum system described in Chapter 1.

Algorithm # 2.1:

1. Choose $Q = diag(q_1, q_2, q_3, q_4)$ as the A matrix is 4×4 matrix, where q_1 corresponds to weight on cart position, q_2 is weight corresponding to cart linear velocity, q_3 is the weight corresponding to the pendulum angle, and q_4 corresponds to the angular velocity.
2. Since, the constraint on cart position is difficult to meet, we choose $q_1 \gg q_2, q_3, q_4$.

3. As the pendulum begins to fall the linear velocity of the cart should change rapidly to prevent this, so $q_2 \gg q_4$.
4. Due to the physical constraints imposed on the pendulum angle and cart position we choose $q_1 \gg q_2, q_3 \gg q_4$.
5. As there is constraint on control we choose $R \gg 1$.
6. Choose $q_1 = 500q, q_2 = 20q, q_3 = 20q, q_4 = q$ and $R = 10^n$.

After several iterations it is found that at the values $q = 100, r = 4$ gives satisfactory performance. The optimal feedback gains are found out to be

$$K_1 = -2.2361, K_2 = -2.7209, K_3 = 17.5208, K_4 = 6.7791 \tag{2.11}$$

The closed loop poles are found out to be $-2.8862 \pm 2.1606i, -2.58 \pm 0.1461i$.

2.3. Results and Discussion

Both, the simulation and experiment are conducted using a second order derivative filter F of cutoff frequency 100 rad/s and damping ratio 0.35. The simulation and experimental results are shown below.

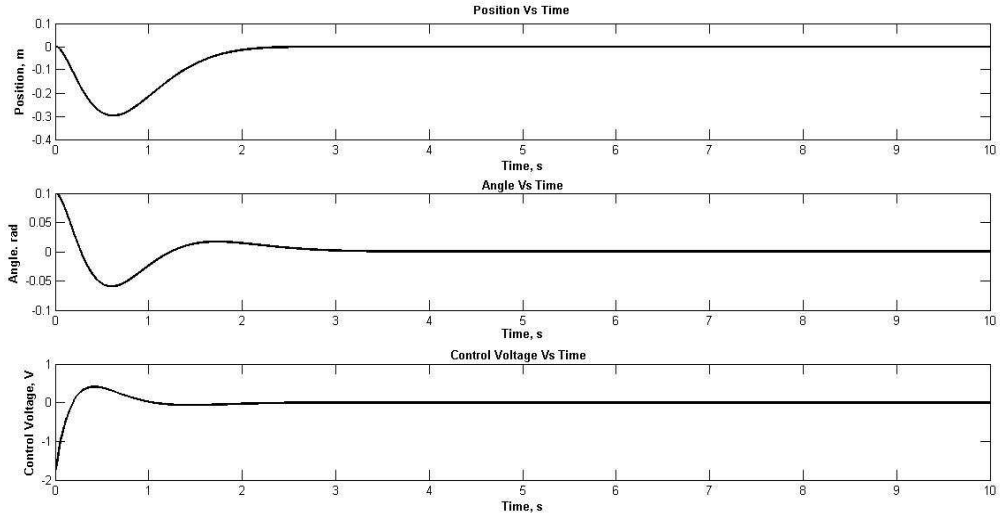

Fig 2.2.LQR state feedback simulation result

The experimental result is obtained as in Fig.2.3. It is seen that the cart position shows undesired oscillations. This may be due to low frequency noise that is not filtered by the filter or due to non-linear friction behavior that causes friction memory like behavior.

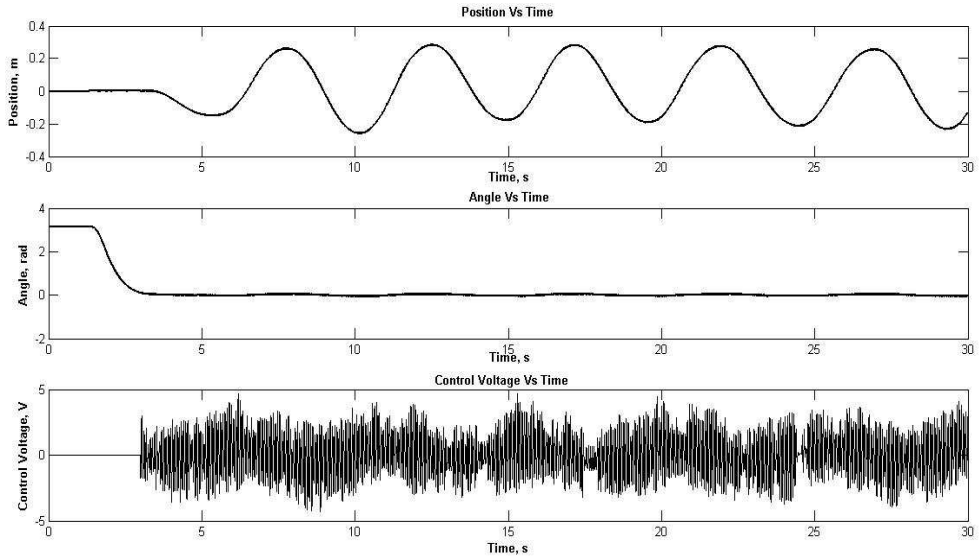

Fig 2.3.Experimental result for LQR state feedback

In order to observe the input side gain tolerability, the gain is decreased and the lower side gain margin of the LQR compensated system is found out.

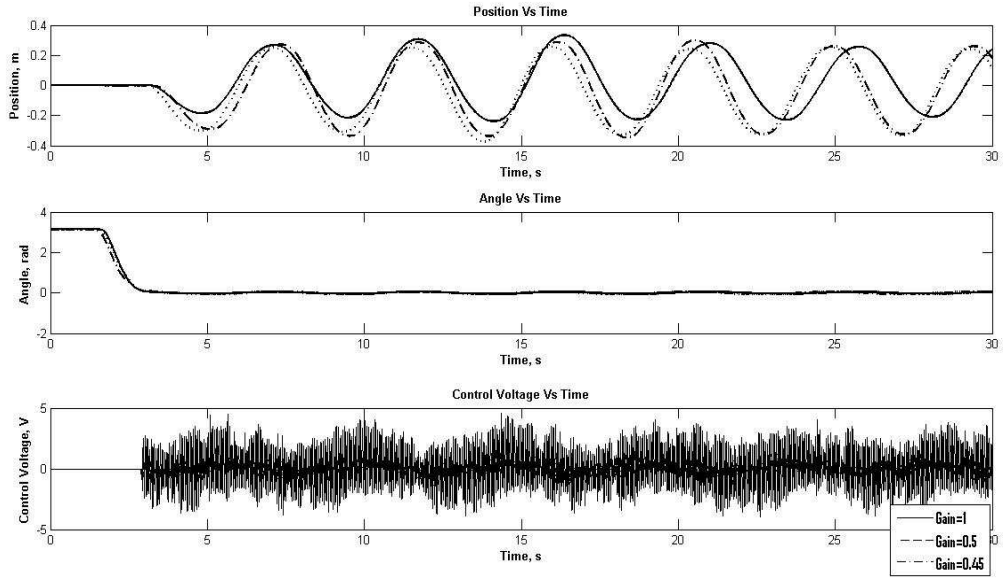

Fig.2.4.Effect of decrease in gain on the LQR compensated system

At a gain of 0.45 it is seen that the system is on the verge of exceeding the track limit. The effect of increase in gain has been given in Fig.2.5.

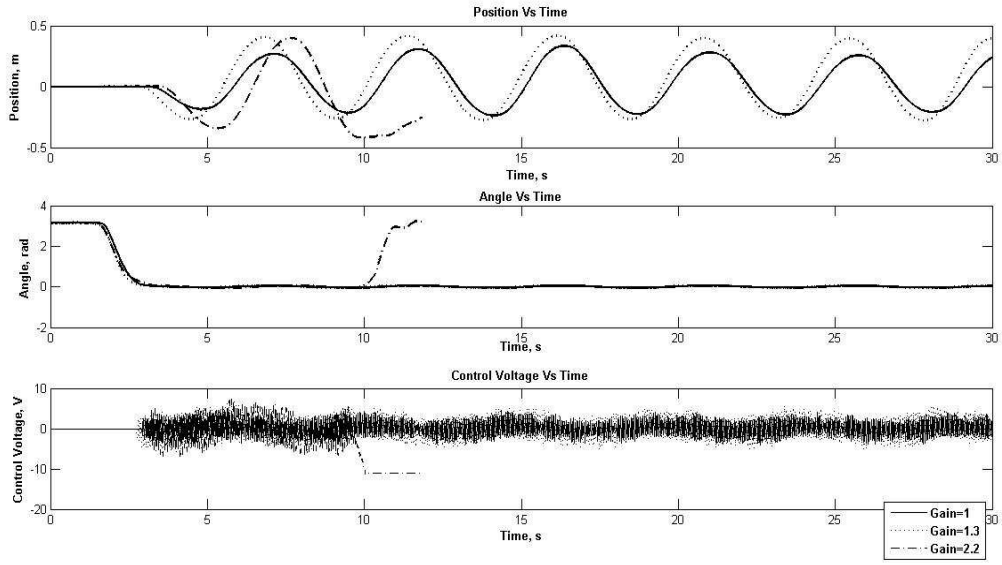

Fig.2.5.Effect of increase in gain on the LQR compensated system

It can be seen that at an input gain perturbation of 2.2 the system becomes just unstable. In Fig.2.6.the effect of delay has been analyzed. This has been done with the help of the transport delay block in SIMULINK, by inserting this block on the input side of the CIPS.

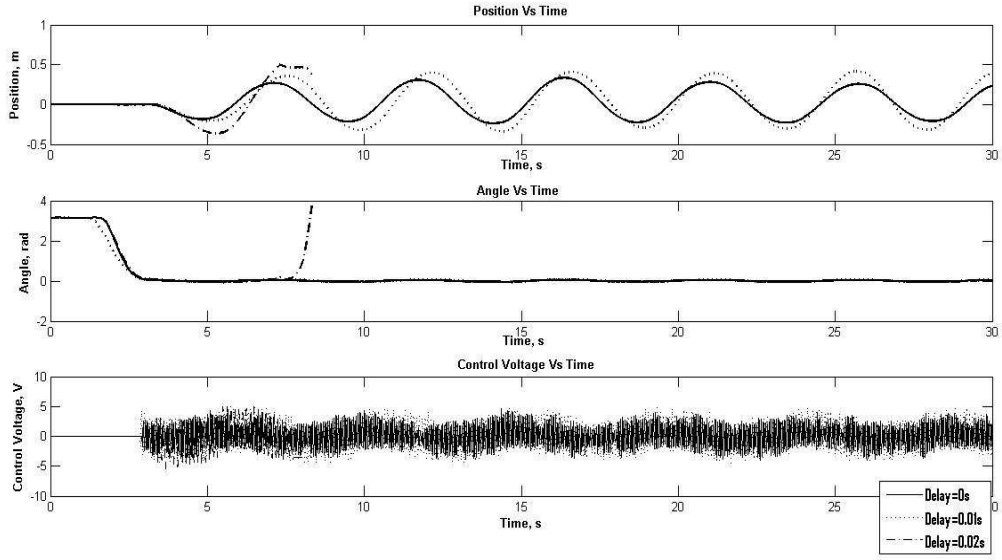

Fig.2.6.Effect of increase in delay on the LQR compensated system

From Fig.2.6. it is evident that the system becomes just unstable just at a delay 0.02s. The multichannel gain perturbation has been analyzed in Fig.2.7.

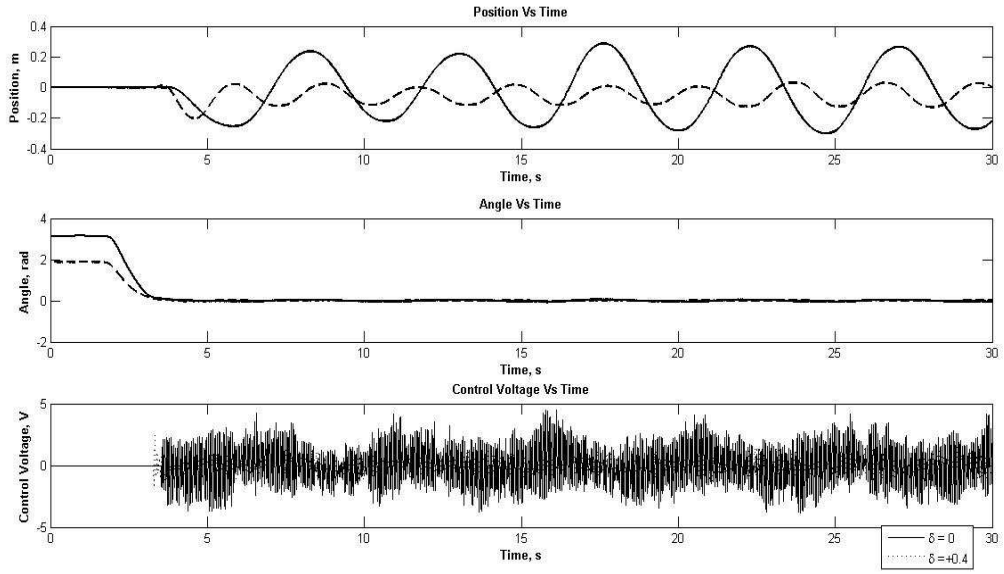

Fig.2.7.Effect of Multichannel gain perturbation on the LQR compensated system

On the output side of the CIPS the effect of gain variation of a multi output system is analyzed with the help of concept of diagonal uncertainty. In this method a gain perturbation of δ is assumed in each channel. A perturbation of $1+\delta$ on the cart position channel and $1-\delta$ on the pendulum angle channel is introduced. To study the effect of δ is varied a range from a value less than +1 to a value greater than -1. This range of δ is the tolerable multi channel gain margin.

A summary of the various robustness margins have been summarized into Table 2.1.

Table.2.1.Summary of LQR Controller Robustness Analysis

Environment	**Gain Margin (Lower side, Upper side)**	**Delay Margin (s)**	**Multichannel Gain Perturbation δ**
Simulation	(0.5,4.99)	0.05	(0,0.2)
Experimental	(0.4518,2.18)	0.02	(0,0.4)

It can be inferred from Table 2.1.that the robustness of the control scheme is well in the range of admissible margin of (0.5, 2) gain margin range. The second order filter transfer function is given as

$$F(s) = \frac{10000}{s^2 + 70.7s + 10000} \tag{2.12}$$

2.4. Chapter Summary

The chapter begins with a very basic explanation of the Linear Quadratic Regulator (LQR) how it is employed in stabilization of inverted pendulum problem is justified. Various points that need to be considered in the design of LQR are also provided. Subsequently, the chapter presents an algorithm for selection of LQR weights. The chapter concludes with the simulation and experimental results. Also the robustness analysis is presented.

Chapter 3

Two Loop Proportional Integral Derivative (PID) Controller Design

The PID controllers are hugely popular owing to their simplicity in working. These controllers are also easy to implement with the help of electronic components. There are several PID tuning methods available in literature like Ziegler-Nichols method, relay method for non-linear systems, here a pole placement method is presented.

3.1. Introduction

The concept of feedback has revolutionized the process control industry. The concept of feedback is really simple. It involves the case when two or more dynamic systems are connected together such that, each system affects the other and the dynamics is strongly coupled. The most important advantage of feedback is that it makes the control insensitive to external disturbances and variation of parameters of system.

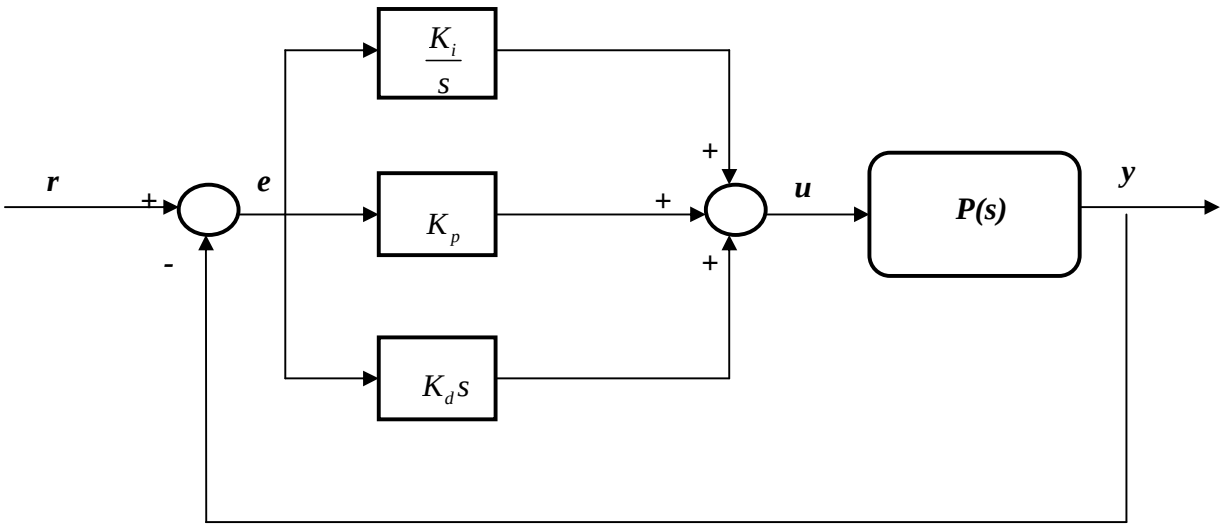

Fig.3.1. Simplified Structure of a PID feedback control system

The control signal u is entirely based on the error generated e. The command input r is also called the set-point weighting in process control literature. The mathematical representation of the control action is [47]

$$e = r - y$$
$$u = K_p e + K_i \int e \ dt + K_d \frac{de}{dt} \tag{3.1}$$

It is seen that with the increase in the value of proportional gain K_p the value of error becomes greatly reduced but the response becomes highly oscillatory. But, with a constant steady state error. Integral term K_i ensures that the steady state error is zero, i.e. the process output will agree with the reference in its steady state. But, large values of the integral gain would make the control input sluggish leading to unsatisfactory performance. The role of the derivative gain K_d is to damp the oscillatory behavior of the process output. Use of high value of K_d may lead to instability. So, in order to achieve satisfactory performance we need to choose these values wisely. There exist many tuning rules out of which Ziegler-Nichols tuning is the most popular one.

Initially, the on-off type of feedback control was widely used. But, due to high oscillatory nature of output response the on-off type feedback controller and due to overreaction of control action, gave way to the P type controller. The control action in the case of P type feedback will be directly proportional to the error generated. A large K_p will reduce sensitivity to load disturbance, but increases measurement noise too. Choice of K_p be is a tradeoff between these two conflicting requirements. It may be noted that the problem of high gain feedback causes instability in closed loop. The upper limit of high gain is determined by the process dynamics.

The Integral action has been a necessary evil in control loops. It has the advantage of guaranteed zero steady state error, but at the cost of sluggish control signal. The derivative action on the other hand improves transient response as it acts on the rate of change of error. It improves the closed loop stability. The choice of K_d is also very crucial, initially increase in its value will increase damping but a high value will eventually decrease the damping.

3.2. Two-loop PID Controller design

It is seen in Chapter 2 that the LQR controller exhibits undesirable sustained oscillations in the cart response that can be prevented in the 2-loop PID controller. The following is the block diagram for the two-loop PID controller for the Inverted Pendulum system is shown in Fig.3.2. The following is the controller structure shown as below, here K_p^1 denotes proportional gain for the controller C_1.

$$C_1 = \frac{K_d^1 s^2 + K_p^1 s + K_i^1}{s} \tag{3.2}$$

$$C_2 = \frac{K_d^2 s^2 + K_p^2 s + K_i^2}{s} \tag{3.3}$$

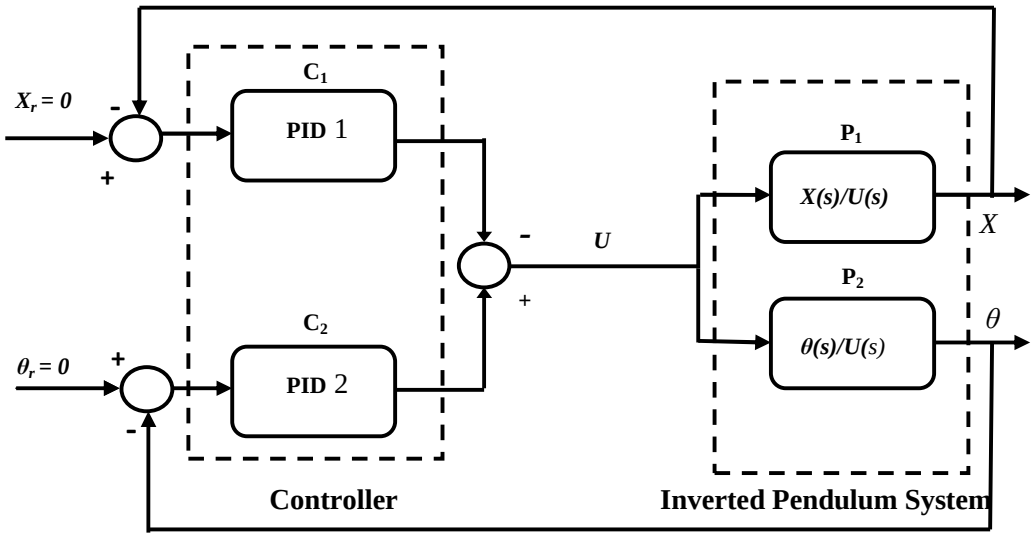

Fig.3.2. Two-loop PID Controller Scheme for the Inverted Pendulum System

Let the plant transfer function be of the form (1.18) and (1.19)

$$\frac{X(s)}{U(s)} = \frac{b_1}{s^2} = \frac{5.841}{s^2} \tag{3.4}$$

$$\frac{\theta(s)}{U(s)} = \frac{b_2}{s^2 - a^2} = \frac{3.957}{s^2 - 6.807} \tag{3.5}$$

The characteristic equation for the two loop PID controller is given as below

$$1 - P_1C_1 + P_2C_2 = 0 \tag{3.6}$$

Substituting the values for P_1, P_2, C_1 and C_2 in (3.6) one obtains the following characteristic equation

$$1 - \frac{b_1}{s^2}\frac{K_d^1 s^2 + K_p^1 s + K_i^1}{s} + \frac{b_2}{(s^2 - a^2)}\frac{K_d^2 s^2 + K_p^2 s + K_i^2}{s} = 0 \tag{3.7}$$

Simplifying (3.7) yields the following equation

$$\begin{aligned} s^5 + (-b_1K_d^1 + b_2K_d^2)s^4 + (-a^2 - b_1K_p^1 + b_2K_p^2)s^3 + (-b_1K_i^1 + a^2b_1K_d^1 + b_2K_i^2)s^2 \\ + (a^2b_1K_p^1)s + (a^2b_1K_i^1) = 0 \end{aligned} \tag{3.8}$$

Since, the characteristic equation is 5^{th} order, it can be compared to the desired characteristic equation of the form

$$s^5 + p_1s^4 + p_2s^3 + p_3s^2 + p_4s + p_5 = 0 \tag{3.9}$$

Comparing (3.8) and (3.9) gives

$$\begin{bmatrix} -b_1 & 0 & 0 & b_2 & 0 & 0 \\ 0 & -b_1 & 0 & 0 & b_2 & 0 \\ a^2b_1 & 0 & -b_1 & 0 & 0 & b_2 \\ 0 & a^2b_1 & 0 & 0 & 0 & 0 \\ 0 & 0 & a^2b_1 & 0 & 0 & 0 \end{bmatrix} \begin{bmatrix} K_d^1 \\ K_p^1 \\ K_i^1 \\ K_d^2 \\ K_p^2 \\ K_i^2 \end{bmatrix} = \begin{bmatrix} p_1 \\ p_2 + a^2 \\ p_3 \\ p_4 \\ p_5 \end{bmatrix} \tag{3.10}$$

Therefore, the two-loop PID Controller design can be converted to a pole placement problem. But, there are six unknowns and five equations thus it is required to choose one variable arbitrarily. This will make the matrix in (3.10) invertible. One can choose the LQR dominant

poles in Chapter 2 for pole placement. It can be seen that the value of K_d^2 can be chosen arbitrarily. Choose $K_d^2 = 10$. We have chosen the desired pole polynomial as

$$s^5 + 26.4s^4 + 218.6s^3 + 871.3s^2 + 1721.8s + 1343.7 = 0 \tag{3.11}$$

The gains of the PID controller are obtained from (3.10) as follows $K_p^1 = 43.3, K_i^1 = 33.796,$ $K_d^1 = 2.254, K_p^2 = 120.9, K_i^2 = 247.3$. Since, ideal PID controllers are not physically realizable as the transfer function is improper; one has to implement it by using a filtered PID; otherwise, the derivative will lead to derivative noise. Various trials were carried out with different values of K_d^2, but it was found that there was no significant improvement in the closed loop system response.

3.3. Result and Discussions

Fig.3.3. presents the simulation results for cart position, pendulum angle and control voltage respectively for an initial angle of 0.1 rad.

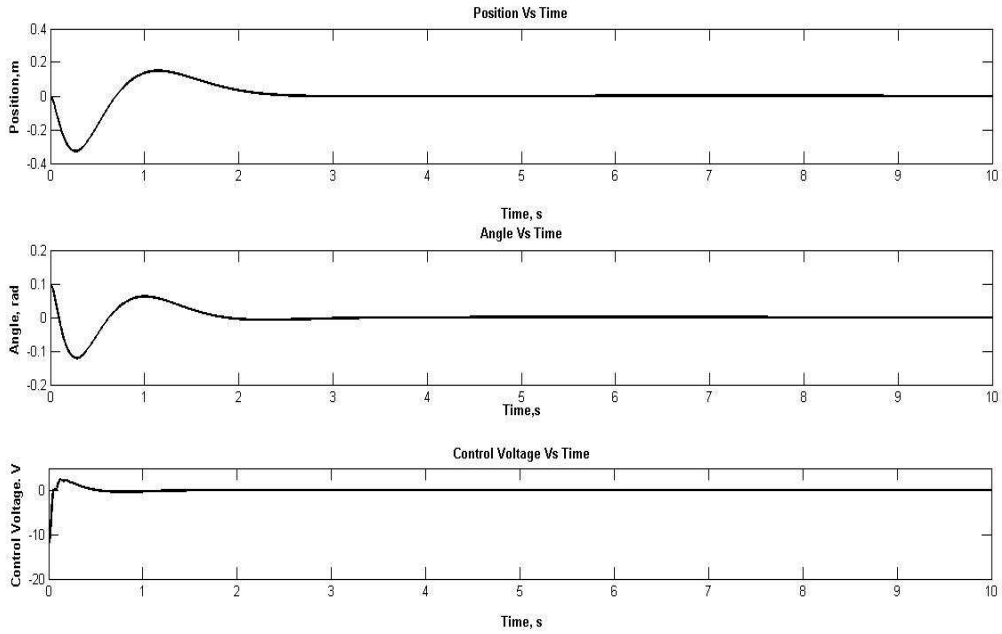

Fig.3.3. Simulation result of Two-Loop PID Controller

The experiment only involves stabilization and no swing up. So the plot of angle begins from 3.14 rad. Fig.3.4 shows the experimental result. It is seen that since the setup is non-linear therefore we have find out the region of attraction is seen that the range of that θ is found that in simulation it is $-0.35\,rad < \theta < 0.35\,rad$ and $-0.48\,rad < \theta < 0.48\,rad$ experimentally. A second order filter having $\xi = 0.35$ and the natural frequency $\omega_n = 100\,rad/s$ is used which gives better sensor noise rejection.

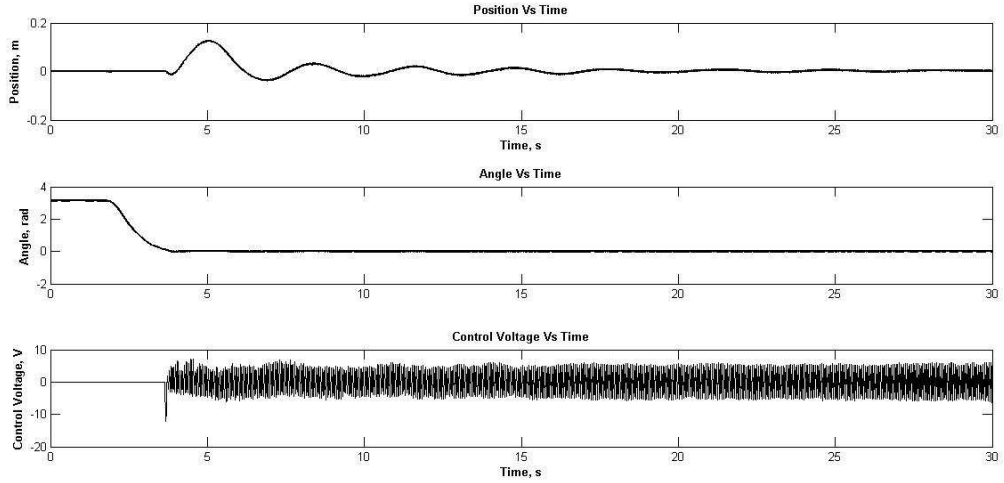

Fig.3.4. Experimental result of Two-Loop PID Controller

Figure 3.5.shows the experimental result for decrease in gain until the system becomes marginally stable. It can be seen that the system gets almost in the verge of breaching the track limit of ± 0.3 m at a decrease in gain of 0.2.

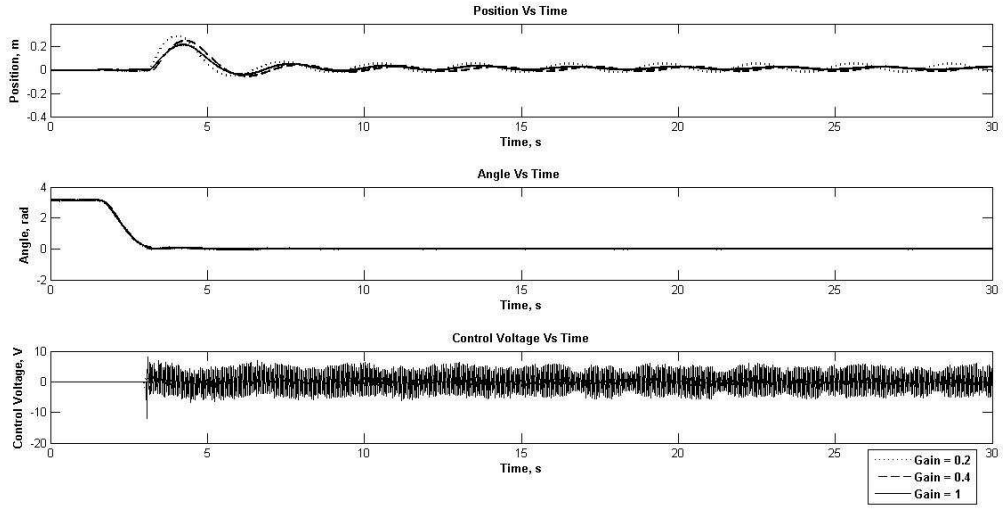

Fig.3.5. Experimental result for decrease in gain

In Figure.3.6.the experimental result for increase in gain has been illustrated. The system cart position exceeds the limit at Gain of 5.

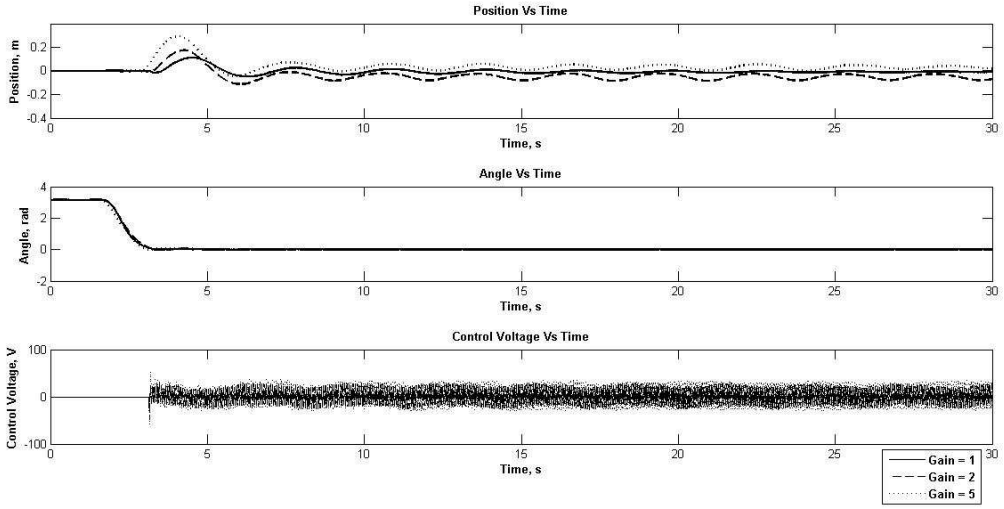

Fig.3.6. Experimental result for increase in gain

In order to determine the phase margin experimentally the concept of delay margin has been utilized. The use of this concept has been implemented in the SIMULINK with the help of transport delay block. Fig.3.7.shows the experimental result for the delay margin analysis.

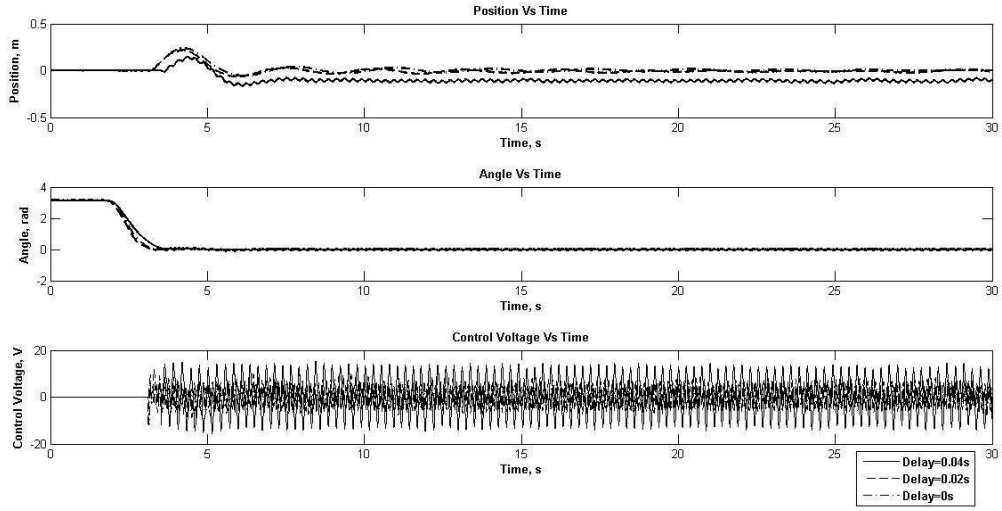

Fig.3.7. Experimental result for increase in delay

It can be seen that the increase in delay causes excessive oscillation in pendulum angle response. These oscillations are also evident in the control voltage response and in the cart position response too

On the output side, we have a multi output system; we have analyzed the effect of gain variation with the help of concept of diagonal uncertainty. In this method we assume that we have a gain perturbation δ in each channel. A perturbation of $1+\delta$ on the cart position channel and $1-\delta$ on the pendulum angle channel is introduced. To study the effect of δ we vary the value of it in a range from a value less than +1 to a value greater than -1. This range of δ is the tolerable multi channel gain margin.

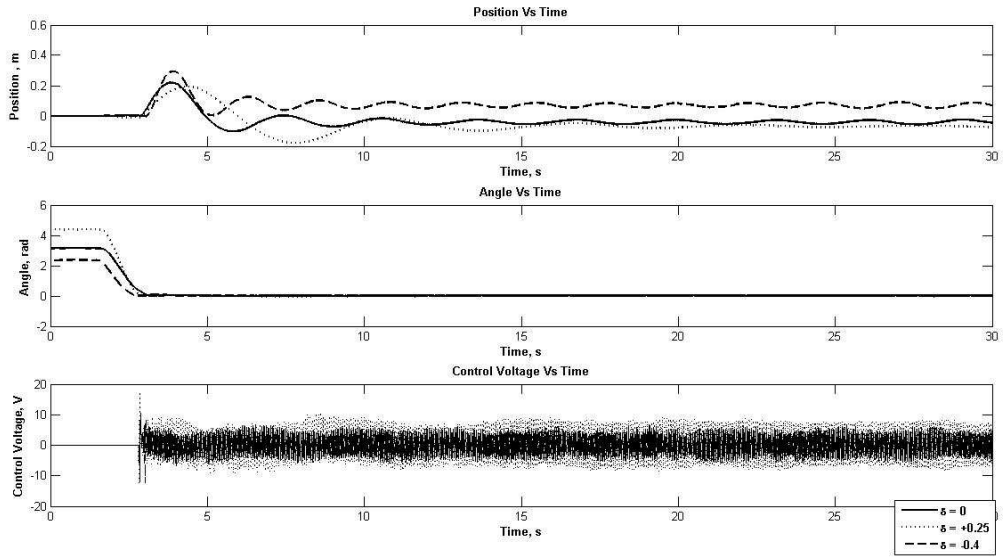

Fig.3.8.Multichannel gain perturbation analysis applied to PID compensation (Experimental)

A summary of the various robustness margins has been summarized into Table 3.1.

Table.3.1.Summary of Robust-2-Loop PID Controller Robustness Analysis

Environment	**Gain Margin (Lower side, Upper side)**	**Gain Crossover Frequency(ω_{gc}) (rad/s)**	**Delay Margin (s)**	**Calculated Phase Margin (deg)**	**Multichannel Gain Perturbation δ**
Simulation	(0.2238,2.2)	27.4	0.034	53.3	(-0.6,+0.174)
Experimental	(0.2,5)	******	0.04	62.7	(-0.4, +0.25)

It can be seen that the robustness of the control scheme is well in the range of admissible margin of (0.5,2) gain margin range and the phase margin 30^{o}.

3.4. Chapter Summary

The chapter introduces the concept of PID control and its relevance in solving practical control issues. Then it develops a method for Two-Loop-PID control design by pole placement. The LQR dominant poles from Chapter 2 are chosen for pole placement. The design is seen to have sufficient nominal robustness.

Chapter 4

Sub-optimal LQR based state feedback subjected to H_∞ constraints

4.1. Introduction

It is very common in control systems to come across requirements that are conflicting among themselves. This can be like rise time, overshoot, gain margin, phase margin etc meeting them simultaneously. Such, contradictory requirements are met by multi-objective optimization. This can be met my methods like convex optimization and genetic algorithms etc. Such a common contradictory optimization encountered in control is that between sensitivity norm and complimentary sensitivity norm. In the next sub section we will explain the two sensitivity norms and their significance.

4.1.1. Robustness

The ultimate aim of all control system designers is to design a control system that will work in the real environment. This means that the system must be less sensitive towards operating conditions, load changes etc. For example in the case of cart-inverted pendulum the system should be less sensitive to external disturbance force applied. In another situation where in the controller must act irrespective of the model uncertainties that might have arisen. The ability of a control system to operate satisfactorily in such realistic situation is called as robustness.

4.1.2. Feedback Properties

The inputs to a typical feedback system in Fig. 4.1. are the reference input *r*, the process disturbance *d*. All the remaining signals can be considered as possible outputs. Various transfer functions can be defined to relate between the various input and output signals.

The system has three transfer function blocks representing the plant *P*, a feedback controller *C* and a feedforward controller *F*. The transfer functions *C* and *F* together define the control law. It is always desired to find out how the error signal *e* is related to the input signals.

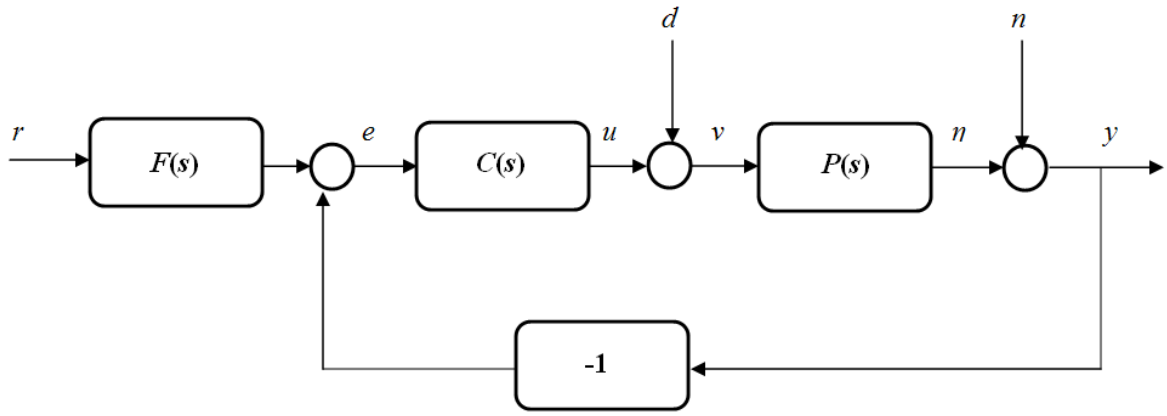

Fig.4.1. Typical schematic for a feedback control system

Transfer functions of a feedback control system are derived under the assumption of that all signals are bounded exponentially. Solving by block diagram reduction, the following equation for *e* can be obtained

$$e = \frac{F}{1+PC} r - \frac{1}{1+PC} n - \frac{PC}{1+PC} d$$
$$= G_{er} r + G_{en} n + G_{ed} d \tag{4.1}$$

4.1.2.1 Sensitivity Functions and Loop goals

From the design point of view it is desirable to analyze the loop transfer function $L = PC$. Ultimately the design procedure is simplified for specifying the design requirements in terms of properties of L. There are two undesirable inputs, one is the load disturbance *d* that makes the output deviate from the reference, while the measurement noise *n* corrupts the information given by the sensors. Thus, the process has three inputs *d*, *n*, *r* and the measured output *y*.

In case of systems where only pure error feedback exists $F = 1$, the system is characterized by the four transfer functions as given below

$$S = \frac{1}{1+PC} = \frac{1}{1+L} \qquad PS = \frac{P}{1+PC}$$
$$T = \frac{PC}{1+PC} = \frac{L}{1+L} \qquad CS = \frac{C}{1+PC} \tag{4.2}$$

Here *PS* is the input sensitivity function (load sensitivity), *CS* is the noise sensitivity function (output sensitivity), *S* is the sensitivity function and *T* is the complimentary sensitivity function. *S* relates between the measured signal *y* and the disturbance input *d*. The complimentary sensitivity function *T* relates between the error signal *e* and the measurement noise *n*. These two are very important in loop design.

The following are the desired loop goals

- Disturbance Rejection- Sensitivity function S must be kept low to minimize the effect of disturbance in output.
- Tracking- Sensitivity function S must be kept low for reducing tracking error.
- Noise Suppression- Complimentary sensitivity function T must be kept small in order to have minimum effect of noise on output and errors.

The most important point that may be noted is that for good tracking and disturbance rejection low *S* is desirable but for good noise rejection low *T* is desired. But both transfer functions add upto unity so both cannot simultaneously be zero. A plot is shown in Fig. 4.2. which depicts the desirable gain plot for the loop transfer function of a feedback control system. The gain crossover frequency ω_{gc} and the slope n_{gc} determine the robustness of the closed loop system. A high value of L at low frequency ensures good load disturbance rejection and excellent tracking properties; a low value of L at high frequency ensures attenuation of high frequency sensor noise. Fig.4.3.shows plots for the sensitivity and complimentary sensitivity transfer functions of loop transfer function.

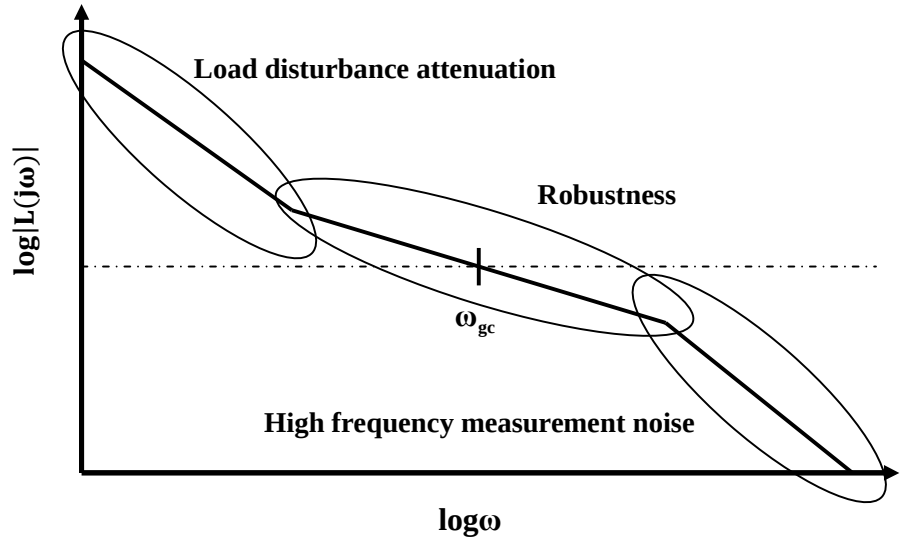

Fig.4.2. Desirable loop gain plot for a feedback control system

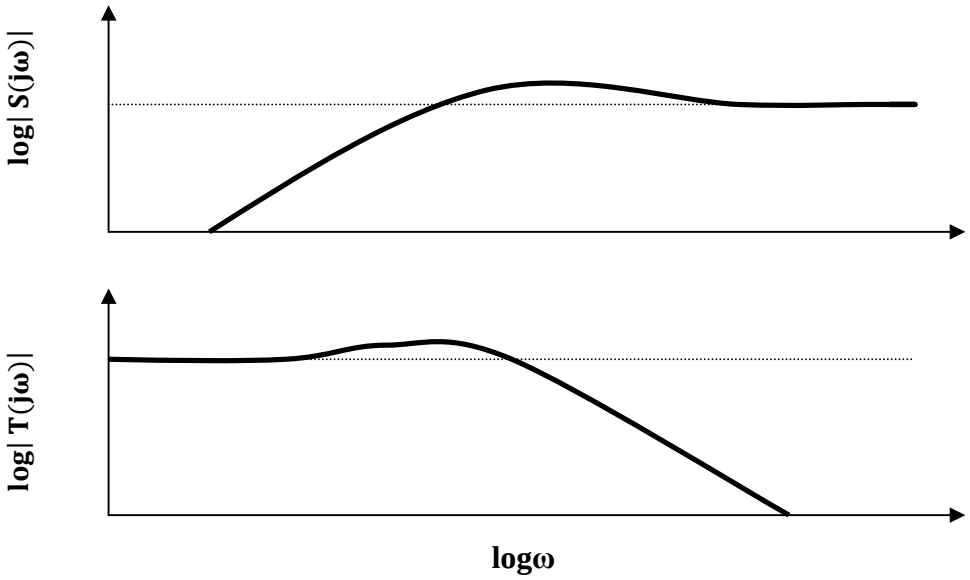

Fig.4.3.Typical Sensitivity Transfer Function S and Complimentary Sensitivity Transfer Function T plots

The crossover region is very critical in case of robustness as this is the region wherein the loop transfer function magnitude changes from values greater than 1 to values less than 1. It is

important to note that in this region neither *S* nor *T* is small. In case of minimum phase plants the poles and zeros can be changed more or less at will to obtain desired *S* and *T* plots. But, in the case of non-minimum phase plants the disturbance rejection ability is limited by bandwidth limitation imposed by the Right Hand Plane zero closest to the origin [48]. In the case of Complimentary sensitivity transfer function *T* bandwidth is limited by the Right Hand Plane pole, it is the frequency above which *T* starts to roll off [48].

4.2. H_∞ Control: A brief review

The H_∞ norm of any transfer function *G(s)* is defined as

$$\left\|G(s)\right\|_\infty = \sup_\omega \left|G(j\omega)\right| \tag{4.3}$$

which is the peak of the Bode magnitude plot of the transfer function. Usually a packed matrix notation to represent the transfer function in state space as given below

$$\begin{aligned} G(s) &= C(sI - A)^{-1}B + D \\ &= \left[\begin{array}{c|c} A & B \\ \hline C & D \end{array}\right] \end{aligned} \tag{4.4}$$

Fig.4.4. depicts a block diagram of the H_∞ control system

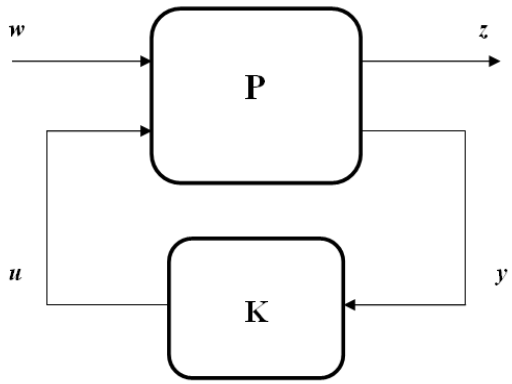

Fig.4.4. Generalized block diagram of H_∞ control system

This generalized structure is used to cast all information about the system into a comprehensive structure. The generalized plant *P* is assumed to be linear and time-invariant, all the required

information including system dynamics, actuator dynamics, perturbation models etc are included in *P*. The sensor measurements providing feedback is given by *y*, the inputs generated by the controller is given by *u*, *w* represents the exogenous inputs to the system that include reference commands, disturbances, sensor noise, fictitious signals that leads to model uncertainties. The signal *z* includes the signals we wish to control which can be performance measure variables, tracking errors, plant outputs and actuator signals that cannot be arbitrarily large and fast. The mathematical representation for the system in Fig.4.4. is as given below

$$\begin{aligned} z &= P_{zw}w + P_{zu}u \\ y &= P_{yw}w + P_{yu}u \\ u &= Ky \end{aligned} \tag{4.5}$$

The closed-loop transfer function between regulated outputs and exogenous inputs is obtained as

$$y = P_{yw}w + P_{yu}Ky \tag{4.6}$$

On solving for *y* in (4.6) and finding *u* in (4.5) terms of *w* gives

$$u = Ky = K(1 - P_{yu}K)^{-1}P_{yw}w \tag{4.7}$$

The general control problem can be defined in this framework is to synthesize a controller such that to keep the value of *z* signal low in the presence of exogenous inputs *w*. If we choose *z* such as those variables that we want to keep low in the presence of external disturbance. Thus, the control problem would reduce to one in which we would like to reduce the "size" of $T_{zw}(s)$ small as possible. Inorder to measure the "size" of any transfer matrix in physically meaningful sense we use the H_∞ norm. This is the most commonly used measure as the H_∞ norm gives the largest possible amplification over all frequency ranges for a unit sinusoidal input signal, or in other words it gives the largest possible energy increase between the input and output of a given system [45].

By using equations from (4.5) to (4.7), $T_{zw}(s)$ can be obtained as

$$T_{zw} = P_{zw} + P_{zw}K(1 - P_{yu}K)^{-1}P_{yw} \tag{4.8}$$

The above expression is called as Linear Fractional Transformation (LFT) of P and K. The plant can also be represented by the following form

$$\begin{aligned} \dot{x} &= Ax + B_1 w + B_2 u \\ z &= C_1 x + D_{11} w + D_{12} u \\ y &= C_2 x + D_{21} w + D_{22} u \end{aligned} \tag{4.9}$$

The packed matrix notation for $P(s)$ is given by

$$P(s) = \left[\begin{array}{c|cc} A & B_1 & B_2 \\ \hline C_1 & D_{11} & D_{12} \\ C_2 & D_{21} & D_{22} \end{array}\right] \tag{4.10}$$

4.3. Linear Matrix Inequalities: Brief Introduction

A Linear Matrix Inequality (LMI) is of the form [49]

$$F(x) \triangleq F_o + \sum_{i=1}^{m} x_i F_i > 0, \tag{4.11}$$

Where $x \in R^m$ is the variable and the matrices $F_i = F_i^T \in R^{n \times n}, i = 0, ..., m$ are given. The inequality sign in (4.11) means that $F(x)$ is positive definite.

Nonlinear (Convex) Inequalities are converted into LMI using Schur compliment defined by the Lemma #4.1.

Lemma # 4.1. Schur Lemma

The LMI as given below

$$\begin{bmatrix} Q(x) & S(x) \\ S(x)^T & R(x) \end{bmatrix} > 0 \tag{4.12}$$

where $Q(x) = Q(x)^T, R(x) = R(x)^T$ and $S(x)$ depends affinely on x is equivalent to

$$R(x) > 0, \; Q(x) - S(x)R(x)^{-1}S(x)^T > 0 \tag{4.13}$$

Or in other words any matrix inequality of the form in (4.13) can be represented as in (4.12).

The LMI equation in (4.11) gives rise to two kinds of questions

- The LMI *feasibility problem* amounts to testing whether there exists real variables $x_1, \ldots\ldots, x_n$ such that (4.11) holds.
- The LMI optimization problem amounts to minimizing the cost function $c(x) = c_1 x_1 + \cdots\cdots c_n x_n$ over all $x_1, \ldots\ldots, x_n$ that satisfy the constraint in (4.11).

The classical linear programs fit into this format easily. The quadratic programs and some cases of convex quadratically constrained quadratic programs can be reformed into this setting. In the case of control, most of the LMIs involve matrix variables than vector variables. That means that most of the inequalities can be considered of the form

$$F(x) > 0 \tag{4.14}$$

Where $F(x)$ is an affine function of the form $F(x) = F_o + T(x)$ and F_o is fixed and $T(x)$ is a linear map. Thus affine functions are linear maps plus some offset.

Various design specifications are converted into LMI constraints to be used in State feedback Control design.

4.4. LMI Formulation for LQR

The LQR control problem has been dealt in detail in Chapter 2. In this section we try to recast the same problem is recast to deal with multi-objective constrained optimization.

For an LTI system

$$\begin{aligned} \dot{x} &= Ax + Bu \\ y &= Cx \end{aligned} \tag{4.15}$$

The LQR Performance index is

$$J = \int_0^\infty (x^T Q x + u^T R u)\ dt \tag{4.16}$$

The problem amounts to finding an optimal state feedback gain K. The cost depends on the trajectory of $x(t)$ so the problem would be to find out the worst possible J for the worst case of $x(t)$ i.e., to find out the optimal cost ${x_o}^T P x_o$.

LMI # 1 Linear Quadratic Regulator

Statement: The LQR control problem is rephrased into an LMI as $\min (x^T(0)\hat{P}^{-1}x(0))$ subject to

$$\begin{bmatrix} A\hat{P}+\hat{P}A^T+BY+Y^TB^T & \hat{P} & Y^T \\ \hat{P} & -Q^{-1} & 0 \\ Y & 0 & -R^{-1} \end{bmatrix} \leq 0, \hat{P}>0 \tag{4.17}$$

where $Y=-K\hat{P}$ and $\hat{P}=P^{-1}$

Proof

The LQR problem is recast into the following objective $\min (x^T(0)Px(0))$ subjected to

$$P>0,\ (A-BK)^TP+P(A-BK)+Q+K^TRK\leq 0 \tag{4.18}$$

Since $P>0,$ consequently $\hat{P}>0$ so that

$$P=\hat{P}^{-1},\ K=-Y\hat{P}^{-1} \tag{4.19}$$

Substituting $\hat{P}$ and Y instead of P and K in (4.18) we get the following

$$\hat{P}A^T+Y^TB^T+A\hat{P}+BY+\hat{P}Q\hat{P}+Y^TRY\leq 0,\ \hat{P}>0 \tag{4.20}$$

Applying Schur Lemma (Lemma # 4.1) we get

$$\begin{bmatrix} A\hat{P}+\hat{P}A^T+BY+Y^TB^T & \hat{P} & Y^T \\ \hat{P} & -Q^{-1} & 0 \\ Y & 0 & -R^{-1} \end{bmatrix} \leq 0, \hat{P}>0 \tag{4.21}$$

In many practical problems it is always advisable to solve for a sub-optimal LQR design wherein the cost is to be minimized below a specified value γ. This problem is stated as a matrix inequality as

$$x^T(0)\hat{P}^{-1}x(0) \le \gamma \tag{4.22}$$

By applying Schur Lemma again we get the LMI

$$\begin{bmatrix} \gamma & x^T(0) \\ x(0) & \hat{P} \end{bmatrix} \ge 0 \tag{4.23}$$

By solving the LMIs in (4.21) and (4.23) simultaneously a sub-optimal LQR solution is obtained.

4.5. LMI Formulation for H_∞

It is well known that the H_∞ norm of a transfer function measures the system input-output gain for finite energy. Or in other words it gives the Largest Singular Value Norm for a finite Root Mean Square (RMS) input signal across frequency in singular value norm. This constraint is helpful in realizing good performance in case of parameter uncertainty hence ensures robust stability [50]. For the system in (9) the maximum singular value for the transfer function is given as

$$\left\| T_{zw} \right\|_\infty \le \sigma \tag{4.24}$$

LMI # 2 Bounded Real Lemma

The statement in (24) can be recast as follows

Statement: If the closed loop system in (10) is stable then the inequality in (4.24) can be recast into an LMI as given below [49]

$$\begin{bmatrix} A\hat{P} + BY + \hat{P}A^T + Y^T B^T & \hat{P}B_1 & C^T \\ B_1{}^T\hat{P} & -\sigma I & 0 \\ C & 0 & -\sigma I \end{bmatrix} \le 0 \tag{4.25}$$

where $Y = -K\hat{P}$ and $\hat{P} = P^{-1}$

Proof

For a system if the packed matrix notation is given by [49]

$$T(s) = = \left[\begin{array}{c|c} A & B \\ \hline C & 0 \end{array}\right] \tag{4.26}$$

Let us define a Hamiltonian matrix H such that

$$H = \begin{bmatrix} A & R \\ Q & -A^T \end{bmatrix} \tag{4.27}$$

An Riccati operation on H yields a stabilizing solution X as $X = Ric(H)$ for the Riccati Equation given as

$$A^T X + XA - XRX + Q = 0 \tag{4.28}$$

In order to minimize the H_∞ norm of T it would be enough to minimize the packed system matrix below a particular $\sigma > 0$

$$\left\| C(sI - A)^{-1} B \right\|_\infty < \sigma \tag{4.29}$$

To minimize this it is enough to minimize the bisection over σ.

$\|T\|_\infty < \sigma$ if and only if

$$\lambda_{\max}(T(-s)^T T(s) - \sigma^2 I) < 0 \quad \forall s \in \mathbb{C}^o \tag{4.30}$$

If and only if

$$\det(T(-s)^T T(s) - \sigma^2 I) \neq 0, \quad \forall s \in \mathbb{C}^o \tag{4.31}$$

If and only if

$$\det\left(\left(\begin{array}{cc|c} A-sI & 0 & B \\ -C^TC & -A^T-sI & 0 \\ \hline 0 & B^T & -\sigma^2 I \end{array}\right)\right)\neq 0,\ \ \forall s\in\mathbb{C}^o \tag{4.32}$$

If and only if

$$\det\left(\left(\begin{array}{cc} A & BB^T/\sigma^2 \\ -C^TC & -A^T \end{array}\right)-sI\right)\neq 0\quad \forall s\in\mathbb{C}^o \tag{4.33}$$

If and only if

$$\left(\begin{array}{cc} A & BB^T/\sigma^2 \\ -C^TC & -A^T \end{array}\right) \tag{4.34}$$

has no eigenvalues in $\mathbb{C}^o$ or else it will lead to an internal instability.

The above statement can be stated by the inequality

$$A^T\hat{P}+\hat{P}A+\sigma^{-2}\hat{P}B_w{B_w}^T\hat{P}+C^TC<0,\quad P>0 \tag{4.35}$$

The above inequality can be converted into Schur Lemma and the following LMI can be obtained

$$\left[\begin{array}{cc} A^T\hat{P}+\hat{P}A+C^TC & \hat{P}B_w \\ {B_w}^T\hat{P} & -\sigma^2 I \end{array}\right]<0 \tag{4.36}$$

Applying Schur Lemma to (4.36) one gets

$$\left[\begin{array}{cc} A^TP+PA & PB_w \\ {B_w}^TP & -\sigma I \end{array}\right]+\left[\begin{array}{c} C^T \\ 0 \end{array}\right]\sigma^{-1}\left[\begin{array}{cc} C & 0 \end{array}\right]<0 \tag{4.37}$$

Applying Schur Lemma again to (4.37), replacing the matrices by the closed loop equivalent and substituting $Y = -K\hat{P}$ and $\hat{P} = P^{-1}$.

$$\begin{bmatrix} A\hat{P} + BY + \hat{P}A^T + Y^T B^T & \hat{P}B_w & C^T \\ B_w{}^T & -\sigma I & 0 \\ C & 0 & -\sigma I \end{bmatrix} \leq 0 \tag{4.38}$$

4.6. LMI formulation for maximum control signal

Considering the physical limitation of control signals or else will lead to actuator saturation which is undesirable. The saturation of actuators will lead to undesirable non-linear behavior of the control system. So we consider the following LMI.

LMI # 3 Maximum Control Signal

Statement :If $u_{\max}$ is maximum control signal amplitude of available control signal for all $t \geq 0$

$$\begin{bmatrix} \hat{P} & Y^T \\ Y & u_{\max}^2 \end{bmatrix} \geq 0 \tag{4.39}$$

Proof

Theorem # 1- Quadratic Stability of Invariant Ellipsoids

Statement: Let H denote the ellipsoid centered at origin. It is said to be invariant if

1. For every trajectory x of a dynamic system $x(t_o) \in H$ implies $x(t) \in H$, $\forall t > t_o$.
2. P satisfies $A^T P + PA < 0$

We assume that the control signal is $u = -Kx = -Y^*(\hat{P}^*)^{-1}$ is the solutions to the LMIs in (4.17) and (4.25) and $x^T(0)\hat{P} - 1x(0) \leq 1$. From the theorem of quadratic stability we get the following statement

$$
\begin{aligned}
\max_{t\geq 0}\|u(t)\|^2 &= \max_{t\geq 0}\left\|Y\hat{P}^{-1}x(t)\right\|^2 \\
&\leq \max_{x\in H}\left\|Y\hat{P}^{-1}x(t)\right\|^2 = \max_{x\in H}(Y\hat{P}^{-1/2}\hat{P}^{-1/2}x)^T(Y\hat{P}^{-1/2}\hat{P}^{-1/2}x) \\
&= \max_{x\in H}(\hat{P}^{-1/2}x)^T(Y\hat{P}^{-1/2})^T(Y\hat{P}^{-1/2})(\hat{P}^{-1/2}x) \\
&\leq \lambda_{\max}\left((\hat{P}^{-1/2}x)^T(Y\hat{P}^{-1/2})^T(Y\hat{P}^{-1/2})(\hat{P}^{-1/2}x)\right) \\
&= \lambda_{\max}\left((Y\hat{P}^{-1/2})^T(Y\hat{P}^{-1/2})x^T\hat{P}^{-1}x\right) \\
&\leq \lambda_{\max}\left((Y\hat{P}^{-1/2})^T(Y\hat{P}^{-1/2})\right)\leq u_{\max}^2
\end{aligned}
\tag{4.40}
$$

Applying Schur Lemma to (4.40) we get the LMI

$$
\begin{bmatrix} \hat{P} & Y^T \\ Y & u_{\max}^2 \end{bmatrix} \geq 0 \tag{4.41}
$$

The LMIs in (4.17), (4.25) and (4.39) were solved for the Inverted Pendulum Stabilization Control Problem using the YALMIP toolbox and MATLAB. The next section describes how to obtain the disturbance model for the physical system as of the form in (4.9).

4.7. Perturbation Model for an Inverted Pendulum System

We consider two fictitious disturbance forces applied to the inverted pendulum system one is the disturbance model applied to the pendulum d_p , and a disturbance applied to the cart d_c. Now, we simplify the system model by considering only that these fictitious forces are applied. Let these forces produce a small perturbation $\Delta\theta, \Delta x$ in pendulum angle and cart position respectively. Consider the disturbance schematic in Fig 4.5.

Let us assume that

$$
\begin{aligned}
\tilde{X}(s) &= X(s) + \Delta X(s) \\
\tilde{\theta}(s) &= \theta(s) + \Delta\theta(s)
\end{aligned}
\tag{4.42}
$$

Substituting the values for the transfer functions we get the following equations

$$
\begin{aligned}
\Delta\ddot{x} &= 0.3894 d_c \\
\Delta\ddot{\theta} &= 0.2638 d_p + 6.807\Delta\theta
\end{aligned}
\tag{4.43}
$$

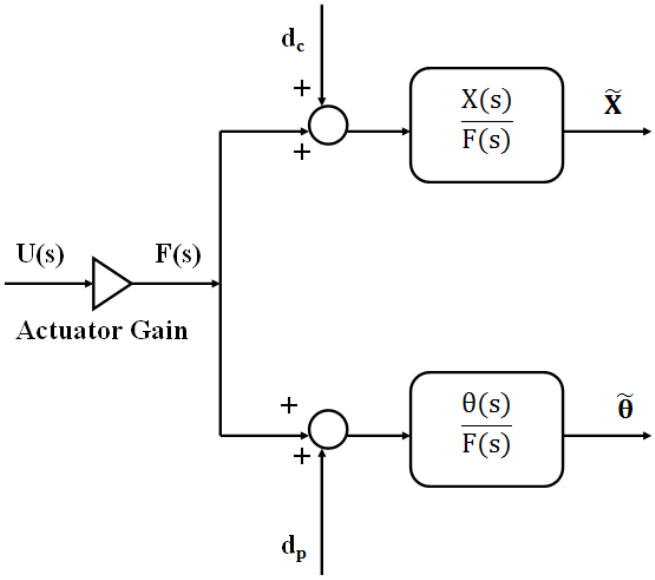

Fig 4.5. Disturbance Model for an Inverted Pendulum System

We assume that $\max(\Delta\theta) = \theta$. Hence, we get the following system matrices

$$A = \begin{bmatrix} 0 & 1 & 0 & 0 \\ 0 & 0 & 0.238 & 0 \\ 0 & 0 & 0 & 1 \\ 0 & 0 & 2*6.807 & 0 \end{bmatrix}, B = \begin{bmatrix} 0 \\ 5.841 \\ 0 \\ 3.957 \end{bmatrix}$$

$$B_W = \begin{bmatrix} 0 & 0 \\ 0.3894 & 0 \\ 0 & 0 \\ 0 & 0.2638 \end{bmatrix}, C = \begin{bmatrix} 1 & 0 & 0 & 0 \\ 0 & 1 & 0 & 0 \\ 0 & 0 & 1 & 0 \\ 0 & 0 & 0 & 1 \end{bmatrix} \quad (4.44)$$

4.8. YALMIP Toolbox: A simplified optimization solver

The YALMIP toolbox was developed by J.Lofberg early in 2001. The semi-definite programming (SDP) and the Linear Matrix Inequalities (LMIs) were the two important contributions to the system and control theory in the last decade [51]. The YALMIP toolbox makes the development of optimization problem in general and control based SDP in particular is simplified. By learning only a minimum of three commands one could get most of the

optimization problems. YALMIP can be flexible solvers of the designers choice. It can be either free solvers or any commercially available solvers. The YALMIP developers a free tutorial on their toolbox in YALMIP/wiki.

4.9. Results and Discussions

In chapter 2, an algorithm and logic for choosing the LQR weights for constrained LQR control problem were presented. We choose $Q = diag([20,30,5,1])$, $R = 1$. The sub-optimal control cost was chosen $\gamma = 100$. The upper bound on the ∞-norm of T was also chosen as $\sigma = 150$. The upper bound on the control signal $u_{\max}$ was chosen as 2V. The above choices obtained a satisfactory system performance.

The following is the solution obtained by using the YALMIP solver

$$K^* = [-13.88, \quad -16.79, \quad 125.35, \quad 34.14] \tag{4.45}$$

And the sub-optimal costs were obtained as $\gamma^* = 50.5143 \ll 100$, $\sigma^* = 72.8 \ll 150$.

The following is the simulation result for an initial pendulum angle of 0.1 rad.

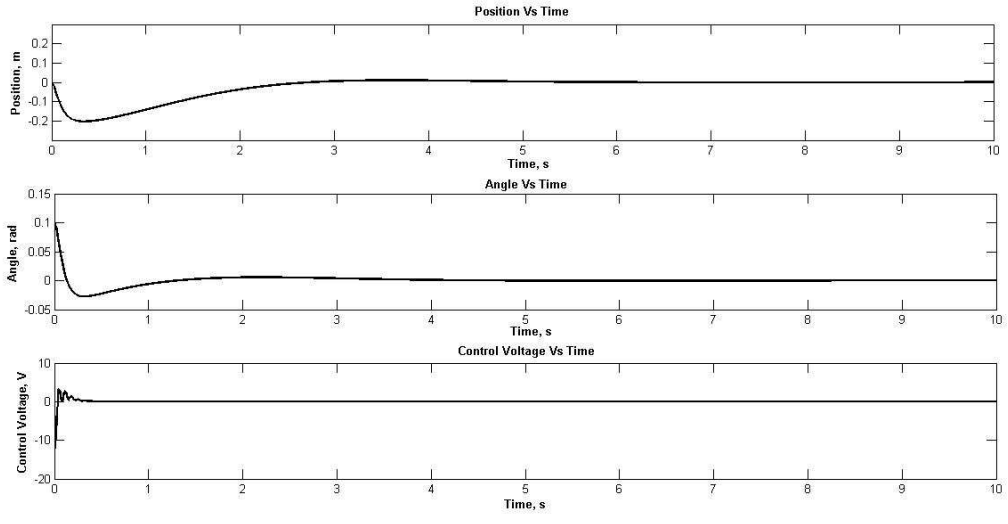

Fig.4.6.Simulation result for the constrained sub-optimal LQR problem

Fig.4.7.shows the experimental results obtained from sub-optimal LQR.

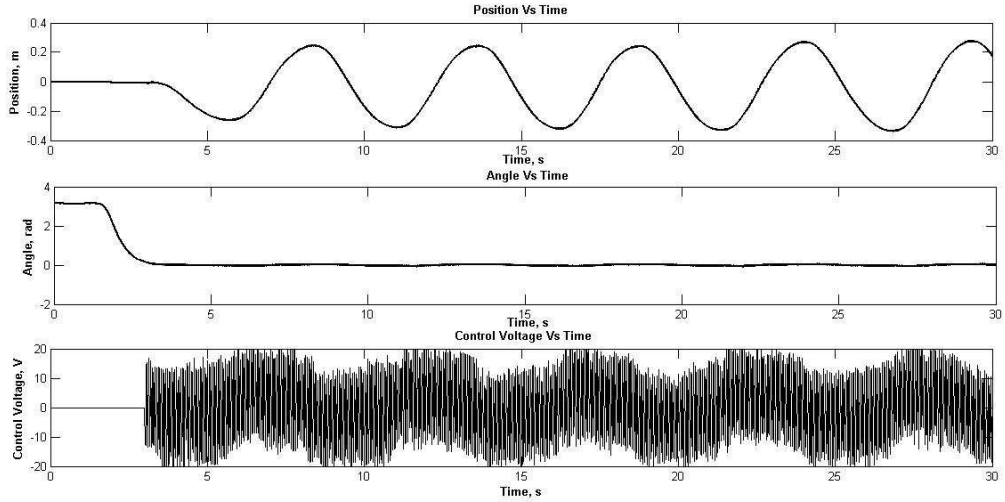

Fig 4.7.Experimental result for the constrained sub-optimal LQR problem

The robustness analysis has also been carried out for this developed scheme. It would be interesting to note that the need to know that, whether the compromise in the LQR cost has given way to better performance in robustness or not in comparison with LQR.

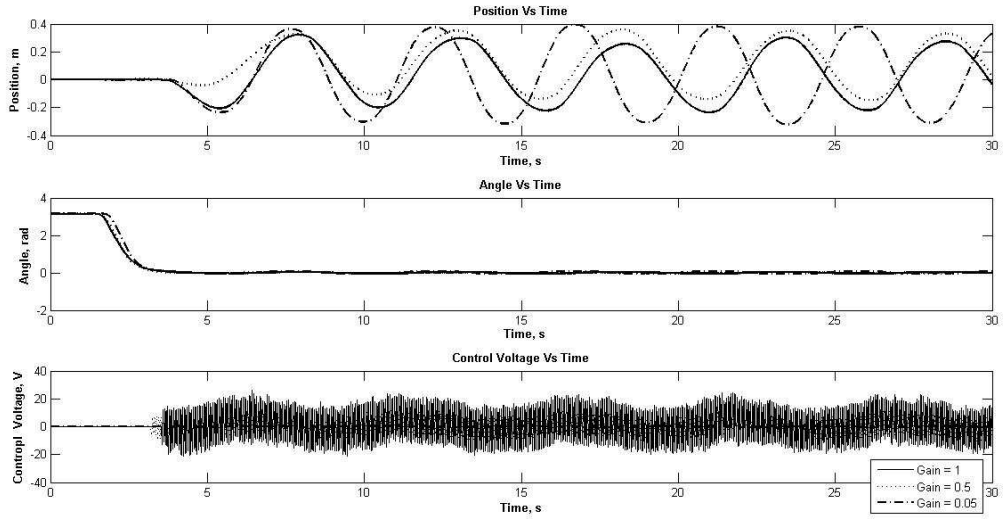

Fig 4.8.Experimental result for decrease in input gain the constrained sub-optimal LQR problem

The system just exceeds the track safety limit at a gain of 0.05 as can be seen in Fig.4.8.

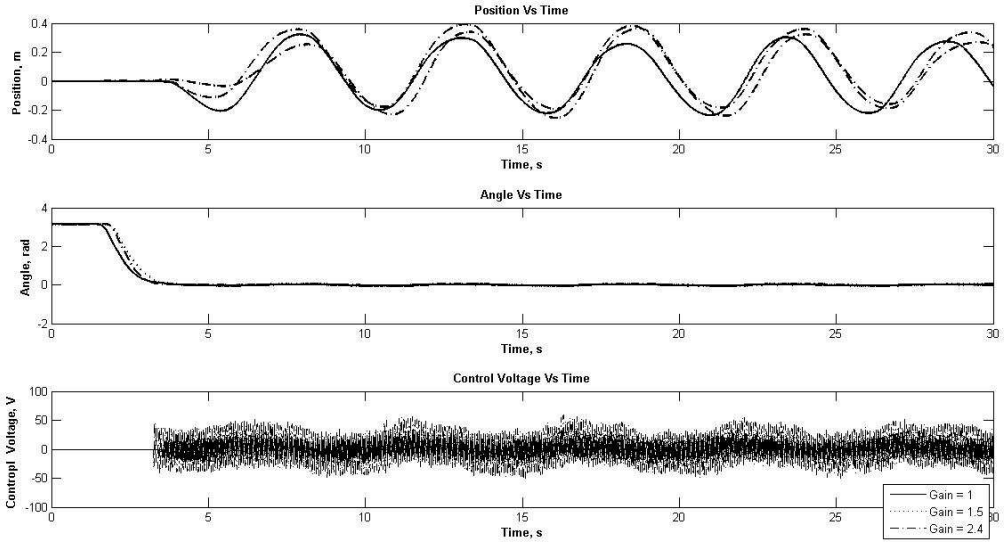

Fig 4.9.Experimental result for increase in input gain the constrained sub-optimal LQR problem

It can be seen in Fig.4.9.that the system breaches the track limit at 0.4 m at a gain of 2.4.The effect of delay has also been analyzed in Fig.4.10. The system is less tolerable to delay in comparison to LQR in Chapter 2. The system becomes unstable at a delay of 0.01s.

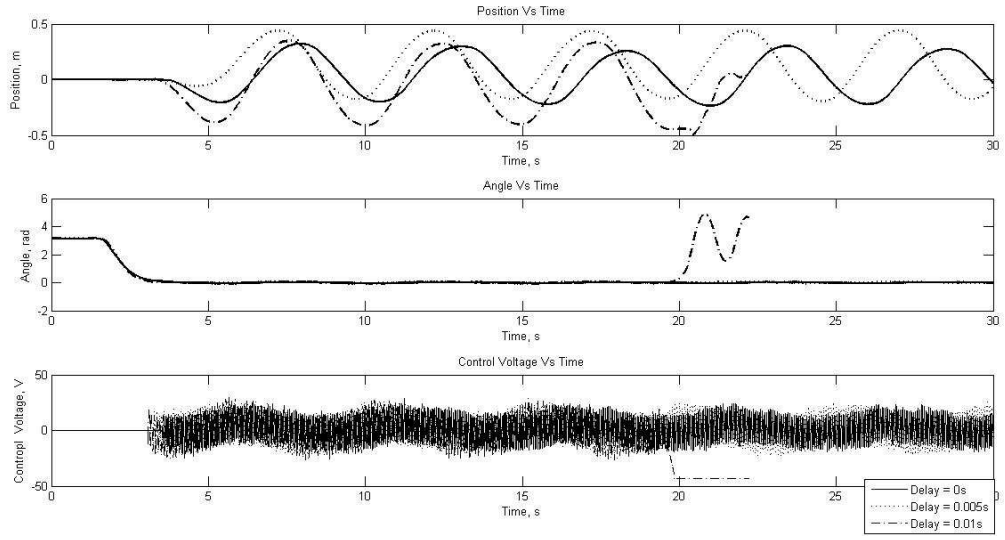

Fig 4.10.Experimental result for increase in input delay the constrained sub-optimal LQR problem

On the output side, we have a multi output system; we have analyzed the effect of gain variation with the help of concept of diagonal uncertainty. In this method we assume that we have a gain perturbation δ in each channel. A perturbation of $1+\delta$ on the cart position channel and $1-\delta$ on the pendulum angle channel is introduced. To study the effect of δ we vary the value of it in a range from a value less than +1 to a value greater than -1. This range of δ is the tolerable multi channel gain margin.

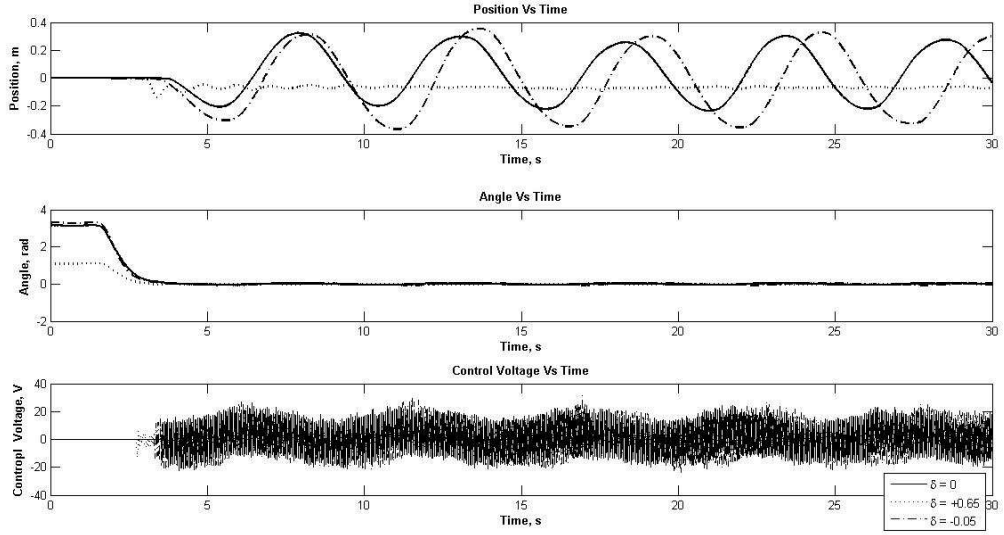

Fig 4.11.Experimental result for output Multichannel gain n the constrained sub-optimal LQR problem

The multi channel tolerability is better than LQR in chapter 2. The robustness analysis has been summarized in Table 4.1.

Table.4.1.Summary of Sub-optimal LQR Robustness Analysis

Environment	**Gain Margin (Lower side, Upper side)**	**Delay Margin (s)**	**Multichannel Gain Perturbation δ**
Simulation	(0.02,1.698)	0.02	(0,+0.17)
Experimental	(0.04,2,39)	0.01	(-.05,+0.065)

4.10. Chapter Summary

The chapter begins with the concept of robustness. The various sensitivity transfer functions are introduced and the design constraints. Then, the chapter explains the concept of H_∞. Since, the sensitivity transfer function and complimentary transfer function are contradictory there is a need for convex optimization using LMIs. A set of three LMIs one for Linear Quadratic Regulator (LQR), second one for H_∞ based on Bounded Real Lemma, and a third one for constraining the control input together with proof. A perturbation model of cart-inverted pendulum is presented. An introduction to YALMIP toolbox is presented which is used to solve the optimization problem. The sub-optimal LQR shows less robustness compared to optimal LQR in Chapter 2 towards loop parameter variations. The chapter concludes with the simulation, experimental and robustness results have been given.

Chapter 5

Integral Sliding Mode (ISM) Controller for the Inverted Pendulum System

5.1. Introduction

The integral action in the sliding mode helps in reducing tracking errors [52].The SMC is known for its good performance in systems with matched uncertainty and disturbances even model uncertainties but at the cost of control chattering and a reaching phase in which the system dynamics is vulnerable towards uncertainties [53]. In most mechatronic systems, it required to have compensation against uncertainties right from the beginning. The ISM offers very good disturbance compensation and retains the full order of the uncompensated system. The next section presents ISM design by pole placement.

5.2. Integral Sliding Mode (ISM) by Pole placement derivation

The integral sliding mode control has several advantages over ideal sliding mode control which are stated as:

- ISM ensures zero steady state error due to inherent integral action.
- Lack of robustness for conventional sliding mode control towards unmatched perturbation
- In the reaching phase conventional sliding mode is sensitive even towards matched perturbation.

The sliding variable in Integral Sliding mode is developed as an integral of output error tracking. The proposed Integral Sliding mode controller achieves system accuracy and robustness. Consider, a dynamical non-minimum phase plant of the form

$$\begin{aligned} \dot{x}(t) &= (A + \Delta A)x(t) + bu(t) + B_w\, w(t) + f(t) \\ &= Ax(t) + bu(t) + \xi(x,t) \\ y(t) &= Cx(t) \end{aligned} \tag{5.1}$$

ΔA is the uncertainty in the plant (A) matrix, $f(t)$ is the unmatched disturbance, $B_w\, w(t)$ is the matched disturbance. The uncertainties can be coupled into a single function $\xi(x,t)$.

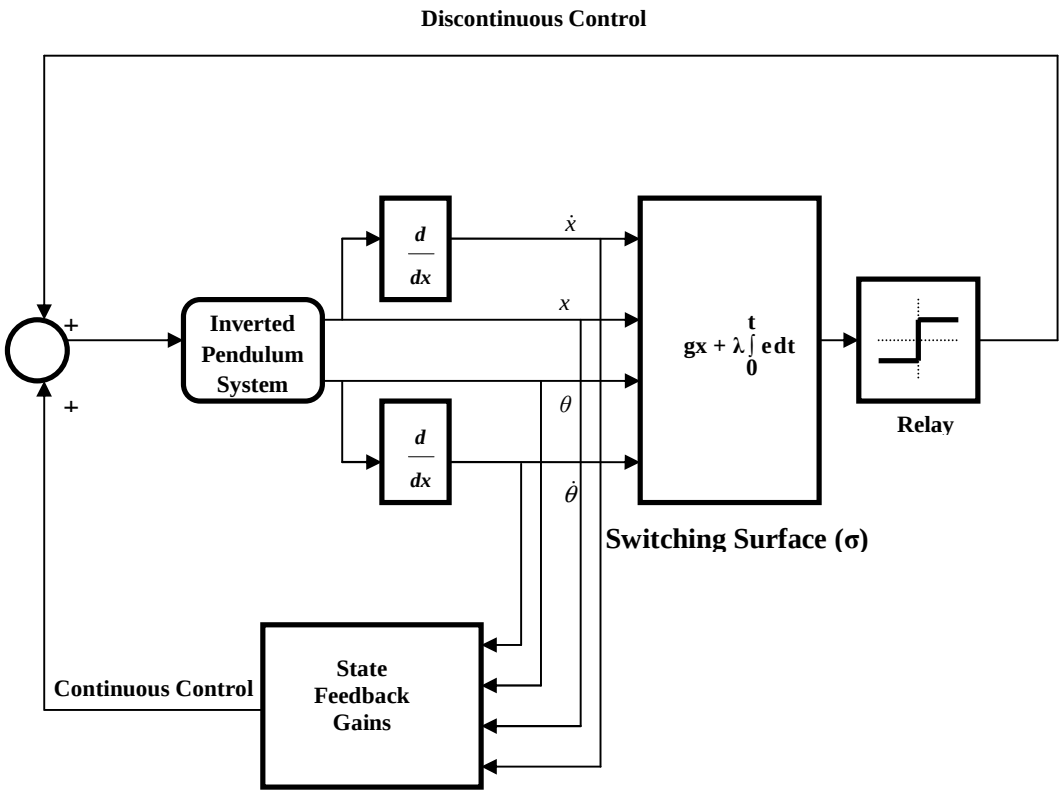

Fig.5.1. Integral Sliding Mode Schematic Block Diagram

Sliding Variable:

***Definition 5.1*:** Let the sliding surface is defined as

$$\sigma(t) = \bar{g}x(t) + \bar{\lambda}\int_0^t \bar{e}\, dt \tag{5.2}$$

where

$$\bar{g} = [g_n \quad g_{n-1} \quad \cdots \quad g_1] \qquad \bar{e} = \begin{bmatrix} y_1 - y_{d1} \\ \vdots \\ y_m - y_{dm} \end{bmatrix}$$
$$\bar{\lambda} = [\lambda_1 \quad \lambda_2 \quad \cdots \quad \lambda_m] \qquad (5.3)$$

For regulator problem $\bar{y}_d = 0$.

Control Signal

$$u = u_O + u_I \qquad (5.4)$$

Equivalent control signal on sliding mode u_O can be obtained for the sliding condition as

$$\dot{\sigma}(t) = 0 \qquad (5.5)$$

Substituting (5.1) and (5.4) in (5.5) one obtains

$$u_O(t) = -\left(\bar{g}b\right)^{-1}\left(\bar{g}Ax(t) + \bar{\lambda}Cx(t) + \bar{g}\xi(x,t)\right) \qquad (5.6)$$

Stability Analysis

The closed loop system is obtained by substituting the equivalent dynamics (5.6) in (5.2)

$$\dot{x}(t) = Ax(t) - b\left(\bar{g}b\right)^{-1}\bar{g}Ax(t) - b\left(\bar{g}b\right)^{-1}\bar{\lambda}Cx(t) + \xi(x,t) - b\left(\bar{g}b\right)^{-1}\bar{g}\xi(x,t) \qquad (5.7)$$

The equivalent closed loop *A* matrix is given as A_{eq}

$$A_{eq} = A - b(\bar{g}b)^{-1}\left(\bar{g}A + \bar{\lambda}C\right) \qquad (5.8)$$

Equation in (5.7) can be modified in the state feedback form as

$$\dot{x}(t) = \left(A + bF_{eq}\right)x(t) + \left\{I_n - b\left(\bar{g}b\right)^{-1}\bar{g}\right\}\xi(x,t) \qquad (5.9)$$

The state feedback F_{eq} can be obtained by pole-placement technique. For stability, we need to ensure that

$$eig\left(A + bF_{eq}\right) < 0 \qquad (5.10)$$

Theorem 5.1.

Assumptions #1.1.: If there exists a known positive constant μ such that

$$\left\|\xi(x,t)\right\| \le \mu \tag{5.11}$$

Where $\left\|(.)\right\|$ denotes the Standard Euclidean norm

Statement: If $\left\|\Gamma(t)\right\| \le \varphi = \left\{I_n - b\left(\overline{g}b\right)^{-1}\overline{g}\right\}\mu$, then the uncertain system in (5.1) is stable boundedly on the sliding surface $\sigma(t) = 0$. The proof of this relation is given in Appendix A.

Equation in (A.6) can be simplified to

$$\dot{V}_1(t) = \lambda_{\min}\left(Q\right)\left\|x(t)\right\|^2 + 2\psi\left\|P\right\|\left\|x(t)\right\| \tag{5.12}$$

Lemma 5.1

If the system in (5.9) if the uncertainty in the system satisfies the matching condition , i.e.

$$rank\left(b \mid \xi(x,t)\right) = rank\left(b\right) \tag{5.13}$$

The system in (5.9) can be simplified into

$$\dot{x}(t) = \left(A + bF_{eq}\right)x(t) \tag{5.14}$$

Let us assume the control law as

$$u(t) = -(\overline{g}b)^{-1}\left\{\overline{g}Ax(t) + \overline{\lambda}Cx(t)\right\} - (\overline{g}b)^{-1}\left(\eta + \alpha\left|\overline{g}\right|\right)\mathrm{sgn}(\sigma) \tag{5.15}$$

Theorem5.2

Statement: The hitting condition is satisfied by the sliding surface $\sigma(t)$ if we can prove that

$$\sigma(t)\dot{\sigma}(t) < -\eta\left|\sigma(t)\right| \tag{5.16}$$

Proof

Let us assume a Lyapunov candidate function provided $\sigma(t) \neq 0$

$$V_2(t) = \frac{1}{2}\left(\sigma(t)\right)^2 \tag{5.17}$$

It is known that the if $\|\xi(x,t)\| \leq \mu$

$$\bar{g}\xi(x,t) \leq \left|\bar{g}\xi(x,t)\right| = \left|\bar{g}\right|\left|\xi(x,t)\right| \leq \left|\bar{g}\right|\mu \tag{5.18}$$

For stability

$$\dot{V}_2(t) < 0 \tag{5.19}$$

We tighten the constraint for finite time reachability of the system trajectory in sliding surface

$$\sigma(t)\dot{\sigma}(t) < -\eta\left|\sigma(t)\right| \tag{5.20}$$

Taking the derivative of the sliding surface

$$\begin{aligned} \dot{\sigma}(t) &= \bar{g}\dot{x}(t) + \bar{\lambda}Cx(t) \\ &= \bar{g}\left\{Ax(t) + bu(t) + \xi(x,t)\right\} + \bar{\lambda}Cx(t) \end{aligned} \tag{5.21}$$

Substituting (5.15) in (5.21) we get

$$\begin{aligned} \dot{\sigma}(t) &= \bar{g}Ax + \bar{g}b\left\{-(\bar{g}b)^{-1}\left\{\bar{g}Ax(t) + \bar{\lambda}Cx(t)\right\} - (\bar{g}b)^{-1}(\eta + \mu\left|\bar{g}\right|)\operatorname{sgn}(\sigma(t))\right\} + \bar{g}\xi(x,t) + \bar{\lambda}Cx(t) \\ &= \bar{g}Ax(t) - \bar{g}Ax(t) - \bar{\lambda}Cx(t) - \eta\operatorname{sgn}(\sigma(t)) - \mu\left|\bar{g}\right|\operatorname{sgn}(\sigma(t)) + \bar{g}\xi(x,t) + \bar{\lambda}Cx(t) \\ &= \bar{g}\xi(x,t) - \eta\operatorname{sgn}(\sigma(t)) - \mu\left|\bar{g}\right|\operatorname{sgn}(\sigma(t)) \end{aligned} \tag{5.22}$$

We now obtain

$$\begin{aligned} \sigma(t)\dot{\sigma}(t) &= \sigma(t)\bar{g}\xi(x,t) - \eta\sigma(t)\operatorname{sgn}(\sigma(t)) - \mu\left|\bar{g}\right|\sigma(t)\operatorname{sgn}(\sigma(t)) \\ &\leq \left|\sigma(t)\right|\left|\bar{g}\right|\mu - \eta\left|\sigma(t)\right| - \mu\left|\bar{g}\right|\left|\sigma(t)\right| = -\eta\left|\sigma(t)\right| \end{aligned} \tag{5.23}$$

Hence the theorem is proved and reachability ensured

Sliding Variable Design by Pole placement

Let us assume that for a SIMO with m outputs the desired characteristic polynomial

$$d(s) = \hat{p}_d(s) + K_1 z_1(s) + \cdots + K_m z_m(s) \tag{5.24}$$

Here $\bar{K} = \begin{bmatrix} K_1 & \cdots & K_m \end{bmatrix}$ and $\bar{G}(s) = \begin{bmatrix} G_1(s) \\ \vdots \\ G_m(s) \end{bmatrix}, G_i(s) = \dfrac{z_i(s)}{\hat{p}(s)}$

If we consider a unity feedback SIMO (Single-Input-Multi-Output) system then the characteristic equation is

$$\Delta(s) = 1 + \bar{K}\left(G(s)\right) \tag{5.25}$$

Theorem 5. 3

Statement: The system poles in (5.9) are identical to the characteristic roots in (5.25)

$$\bar{K} = \bar{\lambda}(\bar{g}b)^{-1} \tag{5.26}$$

Proof

The poles of the system (5.7) by solving the eigenvalues in (5.8)

$$\begin{aligned} d(s) &= \left| sI - A + b(\bar{g}b)^{-1}\left(\bar{g}A + \bar{\lambda}Cx\right)\right| \\ &= \left\{1 + \bar{\lambda}(\bar{g}b)^{-1}\bar{G}(s)\right\} = 0 \end{aligned} \tag{5.27}$$

It can be easily shown that by substituting (5.27) in (5.26)

$$d(s) = 1 + \bar{K}\left(G(s)\right) \tag{5.28}$$

Hence we can show that (5.28) and (5.25) are the same.

The polynomial $\hat{p}(s)$ is the open loop pole polynomial. It should be noted that by the intrinsic property of the sliding mode one pole is always placed in the origin [54], this will also ensure zero steady state property of the sliding mode.

The desired open loop pole polynomial is given by

$$\hat{p}_d(s) = s^n + p_{n-1}s^{n-1+} \cdots + p_1 s \tag{5.29}$$

And associated coefficient vector is

$$\overline{h} = \begin{bmatrix} \hat{p}_1 & \cdots & \hat{p}_{n-1} & 1 \end{bmatrix} \tag{5.30}$$

Lemma 5.2.

Suppose the system in (5.1) is completely controllable then there exists a transformation matrix T such that through the transformation

$$z = Tx \tag{5.31}$$

Where

$$T = \begin{bmatrix} e_n \\ e_n A \\ \vdots \\ e_n A^{n-1} \end{bmatrix},\ M = \begin{bmatrix} b & Ab & \cdots & A^{n-1}b \end{bmatrix}, M^{-1} = \begin{bmatrix} e_1 & e_2 & \cdots & e_n \end{bmatrix}^T \tag{5.32}$$

The system in (5.1) can be transformed into

$$\begin{aligned} \dot{z} &= \hat{A}z + \hat{b}u + T\xi \\ \hat{y} &= \hat{C}z \end{aligned} \tag{5.33}$$

where $\left(\hat{A}, \hat{b}, \hat{C}\right)$ is the controllable canonical form of $\left(A, b, C\right)$.

Theorem 5.4.

Statement: Let the transformation of T be given as in (5.31) and the desired coefficient vector $\overline{h}$ be given as in (5.30) then the transformation is

$$\bar{g} = \bar{h}T \tag{5.34}$$

The polynomial $\hat{p}(s)$ is same as $\hat{p}_d(s)$ in (5.29).

Proof

By using (5.31) and (5.33) in (5.27) we get

$$\begin{aligned}\hat{p}(s) &= \det\left\{sI - T^{-1}AT + T^{-1}b\left(\bar{g}T^{-1}b\right)^{-1}\bar{g}T^{-1}AT\right\} \\ &= \det\left\{sI - \hat{A} + \hat{b}\left(\bar{g}\hat{b}\right)^{-1}\bar{g}\hat{A}\right\}\end{aligned} \tag{5.35}$$

$$\hat{p}(s) = \det\left(sI - \begin{bmatrix} 0 & 1 & 0 & \cdots & 0 \\ 0 & 0 & 1 & \ddots & \vdots \\ \vdots & \ddots & \ddots & \ddots & \vdots \\ 0 & 0 & \cdots & 0 & 1 \\ 0 & -\hat{p}_1 & \cdots & -\hat{p}_{n-2} & -\hat{p}_{n-1} \end{bmatrix}\right) = \hat{p}_d(s) \tag{5.36}$$

5.3. ISM design applied to Cart-Pendulum System

The schematic for ISM applied to Cart-Inverted Pendulum is shown in Fig.5.1. The friction was ideally assumed to be non-existing but, in reality the friction is highly non-linear that may lead to limit cycle like behaviour called as stick-slip oscillations. In order to incorporate this non-linear behaviour we have tried to identify the friction into an exponential friction model as suggested in [55] the linear approach to friction can cause an undesirable unstable, limitcycle like behaviour in practical systems like the speed governors. A basic model for this kind of stick-slip behaviour was also proposed.

5.3.1. Dynamic Cart Friction as an uncertainty in Plant Matrix

The combination of all Coulomb, viscous, static and Stribeck effect can be combined to an exponential form [56] is given by

$$F_{friction} = \begin{cases} F_{static}, \ if \ \ \dot{x} = 0 \\ -\left(\mu_c + \left(\mu_s - \mu_c\right) \mathrm{e}^{\left(-\alpha \dot{x}\right)}\right) F_N \operatorname{sgn}\left(\dot{x}\right) - \varepsilon \dot{x}, \ if \ \ \dot{x} \neq 0 \end{cases} \tag{5.37}$$

Here $\mu_s, \mu_c, \varepsilon$ are the coefficients of static, Coulomb and viscous friction which are estimated experimentally. F_N is the normal force which is the weight of the system. α is the ratio between the form factor and the Stribeck velocity obtained through curve fitting of experimental data

The experiment is conducted under the assumption that friction exists between the cart and the track only. We also assume that the applied voltage is linearly converted into force by the formula

$$F_{applied} = K_{actuator} V \tag{5.38}$$

The details to find out the Coulomb and viscous friction has been given in [56] detail. The pendulum needs to be detached initially due to the above mentioned assumption so that F_N depends only on the cart mass. The method mentioned in [56] was used to find out the $\mu_c = 0.2833$, $\varepsilon \approx 0$ and $\mu_s = 0.043404$. In order, to find out the value of α we need to conduct an experiment by applying a slow varying ramp voltage in one direction so that $\operatorname{sgn}\left(\dot{x}\right) = 1$ and one obtains the corresponding position, filtered velocity and filtered acceleration data shown in Figure 5.2 .

The cart velocity and acceleration data was obtained through differentiation of the position data. Since, the differentiation of output signals generates lot of noise in the data a Butterworth filter of natural frequency $\omega_n = 100 \, rad/s$ and damping ratio 0.35 is used to filter out noisy data. This filter is available in [3]. We have obtained the friction force data by assuming that the friction is the difference between the applied force $F_{applied}$ and the resultant force on the cart obtained by multiplying the cart mass with the instantaneous acceleration.

By using the *Eazyfit* Toolbox® [57], we have obtained the non-linear friction as

$$F_{friction} = -\left(0.2833 + \left(0.043404 - 0.2833\right) \mathrm{e}^{\left(-170 \dot{x}\right)}\right) 23.445 \operatorname{sgn}\left(\dot{x}\right) \tag{5.39}$$

Then we assume that the effect of friction is an anomaly or uncertainty in A matrix. The non-linear equations in (1.6) and (1.7) can be linearized by using Jacobian linearization method we obtain the plant uncertainty matrix ΔA as given in (5.40) by replacing the discontinuity in (5.39) with $\tanh(\dot{x})$.

$$\Delta A = \begin{bmatrix} 0 & 0 & 0 & 0 \\ 0 & 0 & -1.7184 & 0 \\ 0 & 0 & 0 & 0 \\ 0 & 0 & -2.53662 & 0 \end{bmatrix} \tag{5.40}$$

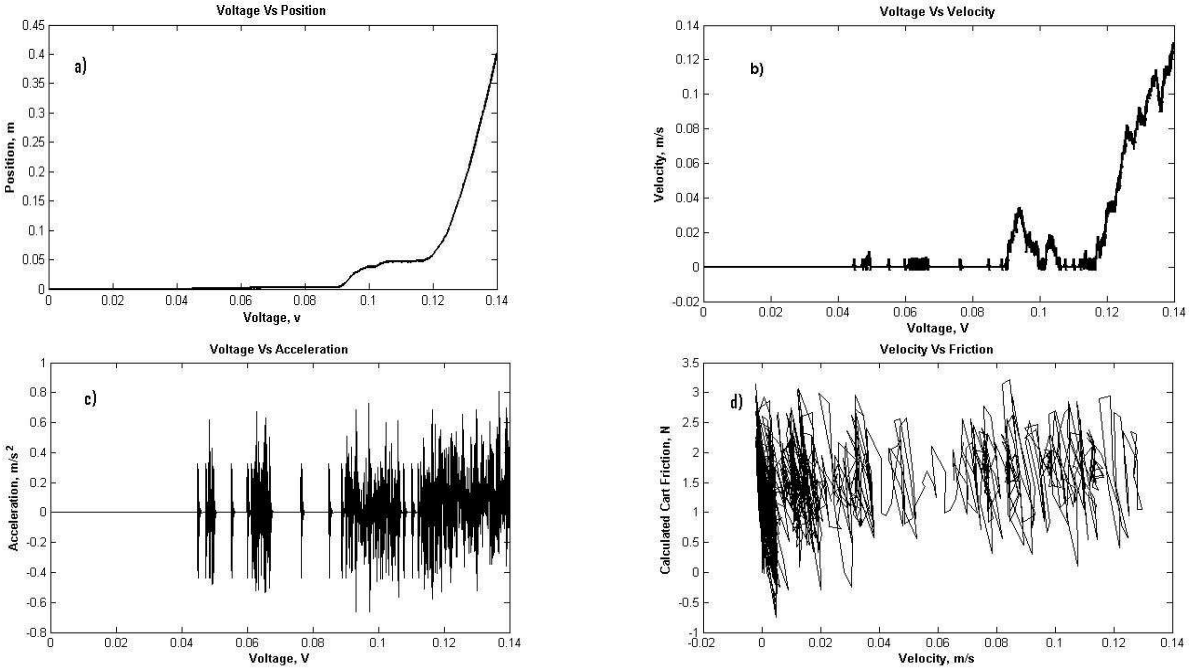

Figure 5.2 (a) Cart position Vs Voltage, (b) Cart Velocity Vs Voltage,(c) Cart Acceleration Vs Voltage, (d) Calculated Cart Friction Vs Velocity

5.3.2. Control Law parameters for Cart-Inverted Pendulum

By using the system state model (1.17), the plant uncertainty matrix(5.40), applying theorems from *Theorem 5.1* to *Theorem 5.4.* ,the complete ISM surface can be obtained as follows

$$\sigma(t) = \begin{bmatrix} -2.7209 & -1.2742 & 6.7791 & 2.1336 \end{bmatrix} \begin{bmatrix} x \\ \dot{x} \\ \theta \\ \dot{\theta} \end{bmatrix} + \int \begin{bmatrix} -2.1831 & 15.4697 \end{bmatrix} \begin{bmatrix} x \\ \theta \end{bmatrix} dt \qquad (5.41)$$

The complete control law is obtained from (5.30), (5.31) and (5.34) as

$$u = \begin{bmatrix} 2.1831 & 2.7209 & -26.4672 & -6.7791 \end{bmatrix} \begin{bmatrix} x \\ \dot{x} \\ \theta \\ \dot{\theta} \end{bmatrix} - 2sat(\sigma(t)) \qquad (5.42)$$

5.4. Results and Discussions

Fig.5.3. gives simulation result (initial angle of 0.1 rad).Figure 5.4 gives the experimental result for the cart-inverted pendulum system. The ISM has been implemented by replacing signum function with saturation which is its continuous approximation in order to reduce chattering. It can be seen in Fig. 5.4. that the cart position has oscillations due to friction memory.

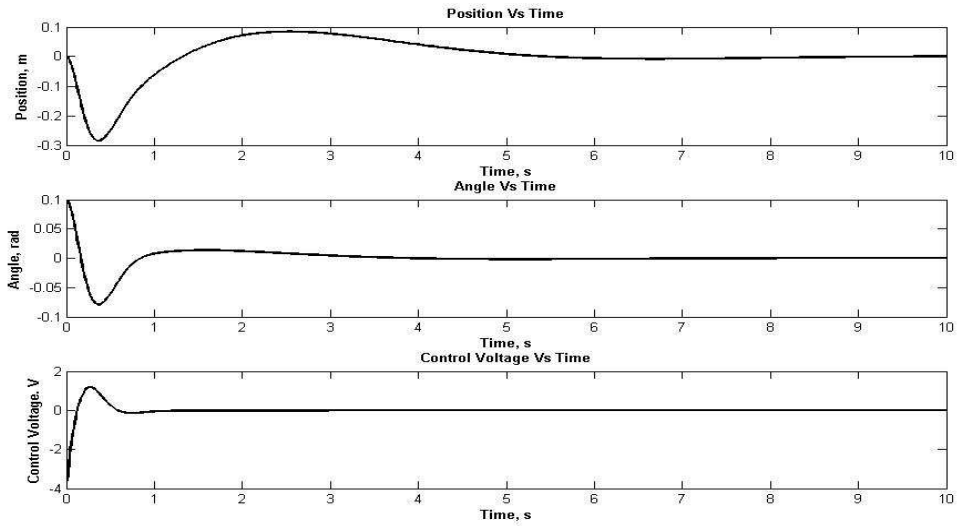

Figure 5.3. Simulation result for ISM applied to Cart-Inverted Pendulum (Initial Angle 0.1 rad)

The ISM is designed by pole-placement by choosing the LQR poles it shows superior performance in terms of more damped cart position oscillatory response. This has been clearly seen from Fig.5.5.

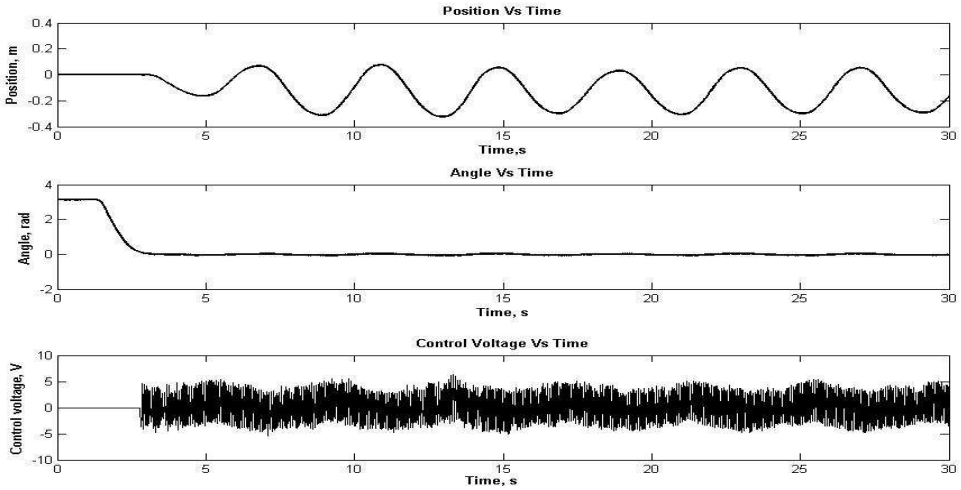

Fig.5.4. Experimental result for ISM applied to Cart-Inverted Pendulum

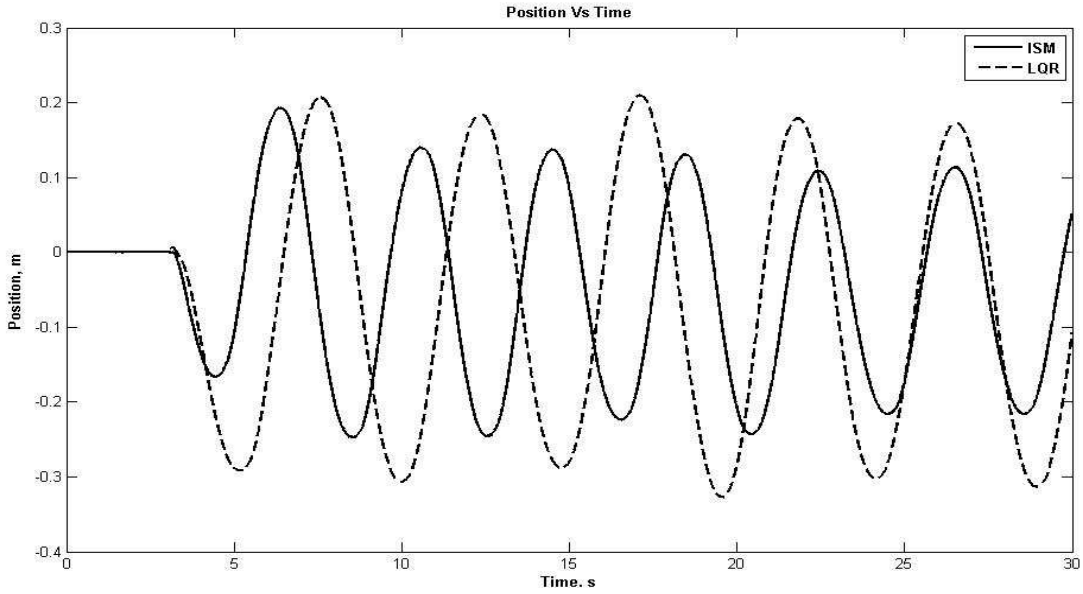

Fig.5.5. Comparison between the cart position responses of ISM and LQR

Fig.5.6.shows the simulation and experimental switching surfaces and phase portraits of the cart position and pendulum angle. From Fig.5.6 (b) it can be seen that there is chattering which is

clearly visible in the experimental switching surface. The effect of discretization of control algorithm can be seen in the Fig.5.6 (d) and Fig.5.6 (f) which are the phase portraits of cart position and pendulum angle respectively

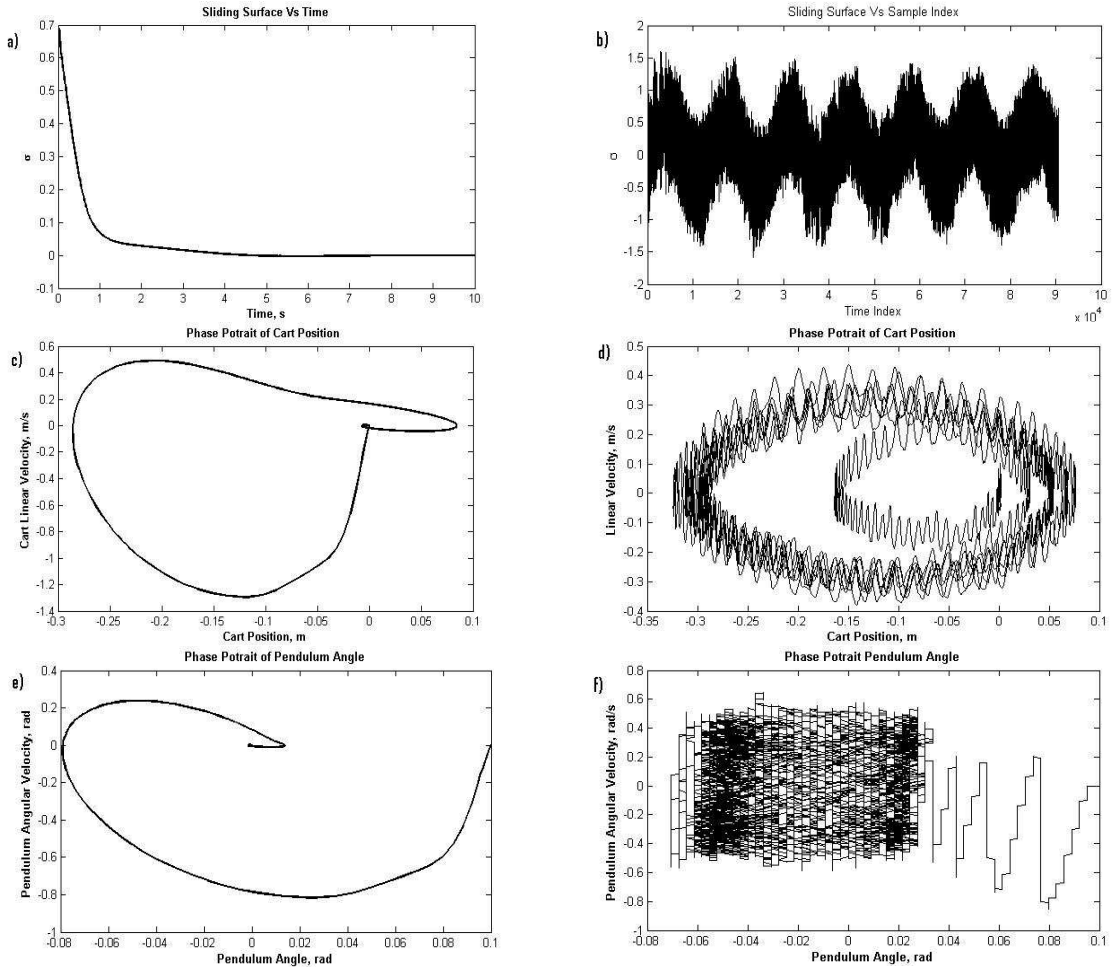

Fig.5.6. Sliding Surface Vs Time in Simulation (a) and Experiment (b), Phase Potrait of Cart Position Simulation (c)and Experiment (d), Phase Potrait of Pendulum Angle in Simulation (e) and Experiment (f)

This chapter also describes the robustness analysis of the designed control scheme. The robustness towards output side multi channel gain perturbation in Fig.5.7.

The range of multichannel gain perturbation δ is of same structure as used in Chapter 2, is obtained as [-0.2, +0.2] from simulation and [-0.15, +0.7] from experiment.

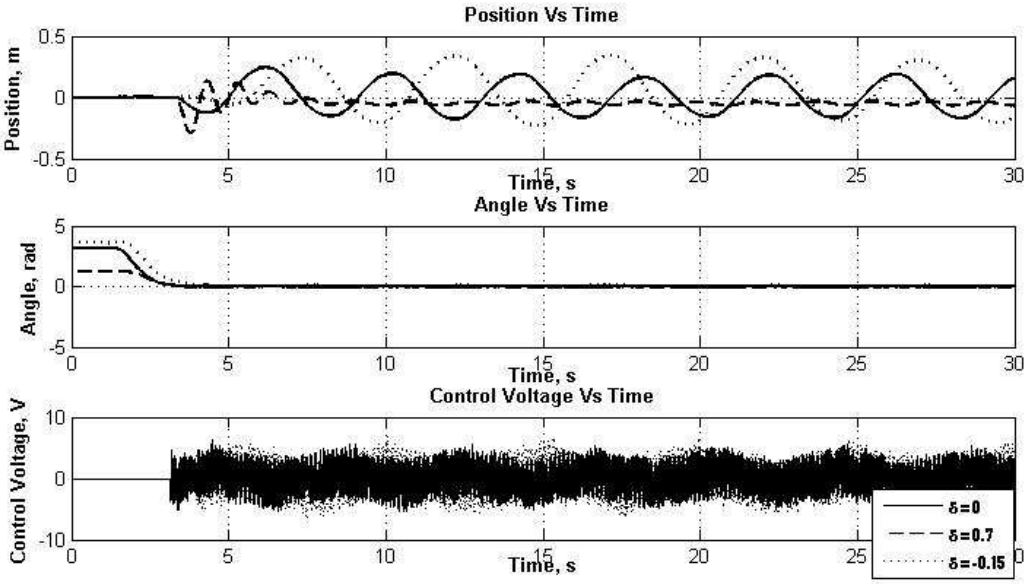

Fig.5.7 .Multichannel Gain Perturbation applied to ISM

5.5. Chapter Summary

The chapter presents the ISM design for cart-inverted pendulum system. The non-linear cart friction is identified into an exponential model and its effect on the plant matrix is modeled as a model uncertainty. The mathematically derived control algorithm for ISM are applied to the cart-inverted pendulum, it shows that compensated system can tolerate more perturbation on the output side when compared to LQR, PID and sub-optimal LQR.

Chapter 6

Conclusions and Suggestions for Future Work

6.1. Conclusions

The thesis presents a number of control approaches such as LQR, Two-Loop PID Controller, Sub-optimal LQR, and ISM. These design methods have been successful in meeting the stabilization goal of the CIPS, simultaneously satisfying the physical constraints in track limit and control voltage. The LQR, Two-Loop-PID and ISM are successful in ensuring good robustness on the input side of the CIPS. The ISM and Two-Loop-PID give good tolerability towards multichannel gain variation on the output side. Due to the non-linear cart friction behavior there is a deviation from the ideal behavior that leads to undesired stick slip oscillations mainly in state feedback based control methods. The Linear Quadratic Regulator (LQR) weight selection for the cart-inverted pendulum has been systematically presented together with robustness analysis. The choice of LQR is well known that unlike ordinary state feedback the LQR solution obtained after LQR weight selection automatically takes care of physical constraints. The LQR poles guarantee minimum robustness of ± 6 dB gain margin and 60^{o} phase margin.

Due to the undesired oscillations in the cart response a Two-Loop-PID controller design was attempted. This approach yielded a nominally robust design with reduced cart oscillations.

A different approach for stabilization through state feedback has been attempted by designing a sub-optimal LQR subjected H_{∞} constraints. As it is well known that the LQR has very poor disturbance rejection property, an H_{∞} constraint might yield a good disturbance rejection. This solution is only possible through a sub-optimal solution.

To increase the robustness in the multichannel output side gain perturbations an Integral Sliding Mode (ISM) controller designed by pole placement method. The ISM poles are placed at the LQR poles, but give superior damped response in cart position.

6.2. Thesis Contributions

The following are the contributions of the thesis

- A systematic algorithm for weight selection for LQR state feedback has been proposed.

- A Two-Loop-PID controller is designed by pole placement approach. The design is based on dominant LQR poles. This has led to improved cart response with damped oscillations.
- A state feedback control design by sub-optimal LQR subjected to H_∞ is designed for cart-inverted pendulum.
- Integral Sliding Mode (ISM) via pole placement algorithm yields better robustness on the output channel than LQR and superior cart position response than LQR.
- Real-time control issues of some of the developed algorithms such as LQR, Two-Loop-PID controller, sub-optimal LQR state feedback subjected H_∞ constraints, ISM have been analysed.
- Since the Two-Loop PID shows damped oscillations in the position response, it is preferable in the case of nominal operation it can be used even under perturbed condition also. This controller also satisfies the nominal robustness.
- In the event of sensor fault the ISM is found to give superior performance.
- Also the robustness of all the developed designs has been verified in simulation and through experiments.

6.3. Suggestions for Future Work

A. Effect of Discretization of Control Algorithm

All the developed designs are implemented in Real Time with the help of SIMULINK and Real-Time Workshop installed in a computer. Since, the computer is digital all the measured signals and the calculated control signals are also digital but this effect of discretization needs on the closed loop system performance also need to be considered in design.

B. Friction Modelling and Advanced Control Design

The non-linear friction model used in Chapter 5 is called as exponential friction model. Other friction models may also be used to identify the non-linear cart friction. This will yield a more accurate non-linear friction model. Further, the friction of the servo mechanism may also be considered. Other advanced control algorithms such as sensitivity weighted LQR and LQR with weighted cost functionals , double integral sliding mode etc., may be attempted.

Appendix A

Statement: If $\|\Gamma(t)\| \le \varphi = \left\{ I_n - b\left(\bar{g}b\right)^{-1}\bar{g} \right\}\mu$, then the uncertain system in (5.1) is stable boundedly on the sliding surface $\sigma(t) = 0$.

Proof:

Let us assume that

$$\begin{aligned} \tilde{A} &= \left(A + bF_{eq} \right) \\ \Gamma(t) &= \left\{ I_n - b\left(\bar{g}b\right)^{-1}\bar{g} \right\}\xi(x,t) \end{aligned} \tag{A.1}$$

We can rewrite (5.9) as

$$\dot{x}(t) = \tilde{A}x(t) + \Gamma(t) \tag{A.2}$$

Let us consider the Lyapunov Function

$$V_1(t) = x^T(t)Px(t) \tag{A.3}$$

P is a solution of the equation in (A.4) and Q is a positive definite symmetric matrix

$$\tilde{A}^T P + P\tilde{A} = -Q \tag{A.4}$$

Derivative of (A.4) gives

$$\begin{aligned} \dot{V}_1(t) &= x^T(t)P\dot{x}(t) + \dot{x}^T(t)Px(t) \\ &= x^T(t)\left\{ \tilde{A}^T P + P\tilde{A} \right\}x(t) + \Gamma^T(t)Px(t) + x^T(t)P\Gamma(t) \end{aligned} \tag{A.5}$$

Substituting (A.4) in (A.5) one obtains

$$\dot{V}_1(t) = -x^T(t)Qx(t) + \Gamma^T(t)Px(t) + x^T(t)P\Gamma(t) \tag{A.6}$$

Equation in (A.6) can be simplified to

$$\dot{V}_1(t) = \lambda_{\min}(Q)\|x(t)\|^2 + 2\psi\|P\|\|x(t)\| \tag{A.7}$$

Since, $\lambda_{\min}(Q) > 0$ which leads to the condition $\dot{V}_1(t) < 0$ for all t and $x \in B^c(\varepsilon)$, where $B^c(\varepsilon)$ is the complement of the closed ball $B(\varepsilon)$ and centred at $x = 0$ with radius given by $\varepsilon = \dfrac{2\varphi\|P\|}{\lambda_{\min}(Q)}$.

Hence the system is boundedly stable.

References

[1] K. J. Astrom, R. M. Murray, "*Feedback systems: An introduction for scientists and engineers*", N J: Princeton University Press, 2008.

[2] "*Digital Pendulum: Installation and Commissioning Manual*", East Sussex, U K: Feedback Instruments Ltd., 2007.

[3] "*Digital Pendulum: Control Experiments Manual*", East Sussex, U K: Feedback Instruments Ltd., 2007.

[4] S. H. Zak, "*Systems and Control*", N Y: Oxford University Press, 2003.

[5] "*Getting Started with Real-Time Workshop ver. 5*", M A: The MathWorks Inc., July 2002.

[6] S. A. Campbell, S. Crawford, K. Morris, "Friction and the Inverted Pendulum Stabilization Problem", *J. of Dyn. Sys., Meas., and Control*, vol.130, no.5, 054502 (7 pages), ASME, August 2008.

[7] B. L. Helourvy, "Stick Slip and Control in Low-Speed Motion", *IEEE Trans. Autom. Control*, vol. 38, no. 10, pp. 1483-1495, Oct 1993.

[8] D. Chatterjee, A. Patra, H. K. Joglekar, "Swing-up and Stabilization of a cart-pendulum system under restricted cart length", *Systems and Control Letters*, vol. 47, pp. 355-364, July 2002.

[9] F. L. Lewis, "Linear Quadratic Regulator (LQR) State Feedback Design", Lecture notes in Dept. Elect. Engineering, University of Texas, Arlington, Oct 2008.

[10] M.G. Henders, A.C. Soudack, "Dynamics and stability state-space of a controlled inverted pendulum", *International Journal of Non-Linear Mechanics*, vol.31, no.2, pp. 215-227, March 1996.

[11] M. W. Dunnigan , "Enhancing state-space control teaching with a computer-based assignment," *IEEE Transactions on Education*, vol.44, no.2, pp.129-136, May 2001

[12] G. W. Van der Linden and P.F Lambrechts, "H/sub ∞/ control of an experimental inverted pendulum with dry friction," *Control Systems IEEE* , vol.13, no.4, pp.44-50, Aug. 1993

[13] S. K. Das, K. K. Paul, “Robust compensation of a Cart–Inverted Pendulum system using a periodic controller: Experimental results”, *Automatica*, vol. 47, no. 11, pp. 2543-2547, November 2011.

[14] C. C. Hung, B. Fernandez, "Comparative Analysis of Control Design Techniques for a Cart-Inverted-Pendulum in Real-Time Implementation," *American Control Conference*, pp.1870-1874, 2-4 June 1993.

[15] K.J. Astrom, K. Furuta, “Swinging up a pendulum by energy control” , *Automatica*, vol. 36, no. 2, pp. 287-295, February 2000

[16] A.S. Shiriaev, O. Egeland, H. Ludvigsen, A.L. Fradkov, “VSS-version of energy-based control for swinging up a pendulum”, *Systems and Control Letters*, vol. 44, no. 1, pp. 45-56, September 2001.

[17] D. Angeli, “Almost global stabilization of the inverted pendulum via continuous state feedback,” *Automatica*, vol. 37, no. 7, Pages 1103-1108, July 2001.

[18] J.P.F. Garcia, J.M.S. Ribeiro, J.J.F. Silva, E.S. Martins, "Continuous-time and discrete-time sliding mode control accomplished using a computer," , *IEE Proceedings - Control Theory and Applications*, vol.152, no.2, pp. 220- 228, March 2005

[19] A.M. Bloch, N.E. Leonard, J.E. Marsden, , "Controlled Lagrangians and the stabilization of mechanical systems. I: The first matching theorem," *IEEE Transactions on Automatic Control*, vol.45, no.12, pp.2253-2270, Dec 2000

[20] B. Srinivasan, P. Huguenin, D. Bonvin, “Global stabilization of an inverted pendulum–Control strategy and experimental verification”, Automatica, vol. 45, no. 1, January 2009, pp. 265-269.

[21] J. Zhao, M.W. Spong, “Hybrid control for global stabilization of the cart–pendulum system,” *Automatica*, vol.37, no.12, pp.1941-1951, December 2001

[22] Q. Wei, W.P. Dayawansa, W.S. Levine, “Nonlinear controller for an inverted pendulum having restricted travel,” *Automatica*, vol. 31, no. 6, pp. 841-850, June 1995

[23] R. Lozano, I. Fantoni, D. J. Block, ”Stabilization of the inverted pendulum around its homoclinic orbit,” *Systems & Control Letters*, vol. 40, no. 3, pp. 197-204, July 2000.

[24] R.F. Harrison, "Asymptotically optimal stabilizing quadratic control of an inverted pendulum," *IEE Proceedings-Control Theory and Applications*, vol.150, no.1, pp. 7- 16, Jan. 2003.

[25] P. J. Gawthrop, L. Wang, “Intermittent predictive control of an inverted pendulum,” *Control Engineering Practice*, vol. 14, no. 11, pp. 1347-1356, November 2006.

[26] C. C. Shiung, C. W. Liang Chen, "Robust adaptive sliding-mode control using fuzzy modeling for an inverted-pendulum system," *IEEE Transactions on Industrial Electronics*, vol.45, no.2, pp.297-306, Apr 1998.

[27] C.-C. Wong, B.-C. Hunag, J.-Y. Chen, , "Rule regulation of indirect adaptive fuzzy controller design," , *IEE Proceedings - Control Theory and Applications*, vol.145, no.6, pp.513-518, Nov 1998.

[28] P. Young-Moon, M. Un-Chul, K.Y. Lee, "A self-organizing fuzzy logic controller for dynamic systems using a fuzzy auto-regressive moving average (FARMA) model," *IEEE Transactions on Fuzzy Systems*, vol.3, no.1, pp.75-82, Feb 1995

[29] H.K. Lam, F.H. Leung, P.K.S. Tam, "Design and stability analysis of fuzzy model-based nonlinear controller for nonlinear systems using genetic algorithm," *IEEE Transactions on Systems, Man, and Cybernetics*, vol.33, no.2, pp. 250- 257, Apr 2003

[30] G. Li, X. Liu, “Dynamic characteristic prediction of inverted pendulum under the reduced-gravity space environments,” *Acta Astronautica*, vol. 67, no.6, pp. 596-604, October 2010.

[31] C.W. Tao, J.S. Taur, C.M. Wang, U.S. Chen, “Fuzzy hierarchical swing-up and sliding position controller for the inverted pendulum–cart system,” *Fuzzy Sets and Systems*, vol. 159, no. 20, pp. 2763-2784, October 2008.

[32] O. Sung-Kwun , P. Witold, R. Seok-Beom, A. Tae-Chon, “Parameter estimation of fuzzy controller and its application to inverted pendulum,” *Engineering Applications of Artificial Intelligence*, vol. 17, no. 1, Pages 37-60, February 2004.

[33] C. Yong-Yan, L. Zongli, "Robust stability analysis and fuzzy-scheduling control for nonlinear systems subject to actuator saturation," *IEEE Transactions on Fuzzy Systems*, vol.11, no.1, pp. 57- 67, Feb 2003.

[34] J. Yi, N. Yubazaki, “Stabilization fuzzy control of inverted pendulum systems, Artificial Intelligence in Engineering,” vol. 14, no. 2, pp. 153-163, April 2000.

[35] T.J. Koo, "Stable model reference adaptive fuzzy control of a class of nonlinear systems," *IEEE Transactions on Fuzzy Systems*, vol.9, no.4, pp.624-636, Aug 2001.

[36] A. Varsek, T. Urbancic, B. Filipic, "Genetic algorithms in controller design and tuning," *IEEE Transactions on Systems, Man and Cybernetics,* vol.23, no.5, pp.1330-1339, Sep/Oct 1993.

[37] C.-C. Chen, C.-C. Wong, "Self-generating rule-mapping fuzzy controller design using a genetic algorithm," *IEE Proceedings - Control Theory and Applications,* vol.149, no.2, pp.143-148, Mar 2002.

[38] D. Del Gobbo, M. Napolitano, P. Famouri, M. Innocenti, "Experimental application of extended Kalman filtering for sensor validation," *IEEE Transactions on Control Systems Technology*, vol.9, no.2, pp.376-380, Mar 2001.

[39] G.W. Irwin, J. Chen, A. McKernan, W.G. Scanlon, "Co-design of predictive controllers for wireless network control," *IET Control Theory & Applications*, vol.4, no.2, pp.186-196, February 2010.

[40] M.E. Magana, F. Holzapfel, "Fuzzy-logic control of an inverted pendulum with vision feedback ," *IEEE Transactions on Education,* vol.41, no.2, pp.165-170, May 1998.

[41] L.K. Wong, F.H.F. Leung, P.K.S. Tam, "Lyapunov-function-based design of fuzzy logic controllers and its application on combining controllers," *IEEE Transactions on Industrial Electronics*, vol.45, no.3, pp.502-509, Jun 1998.

[42] A. Probst, M.E. Magaña, O. Sawodny, "Using a Kalman filter and a Pade approximation to estimate random time delays in a networked feedback control system," *IET Control Theory & Applications*, vol.4, no.11, pp.2263-2272, November 2010.

[43] G. Buttazzo, M. Velasco, P. Marti, "Quality-of-Control Management in Overloaded Real-Time Systems," *IEEE Transactions on Computers*, vol.56, no.2, pp.253-266, Feb. 2007.

[44] J. P. Hespanha, "LQG/LQR controller design", Undergraduate Lecture notes, Department of Electrical and Computer Engineering , University of California, Santa Barbara (UCSB), April 1, 2007.

[45] W. S. Levine, *The Control Handbook: Control System Advanced Methods,* 2nd Edition, Boca Raton, FL: CRC Press, 2011.

[46] K.J. Astrom, T. Hagglund, "The future of PID control," *Control Engineering Practice,* vol. 9, no. 11, pp. 1163-1175, November 2001.

[47] K. J. Astrom, T. Hagglund, "PID Controllers: Theory, Design and Tuning", 2nd Edition, NC: Instrument Society of America (ISA), 1995.

[48] S. Skogestad and I. Postlethwaite, *Multivariable Feedback Control: Analysis and design*, 2nd Edition, Chichester, John Wiley and Sons, 2005.

[49] S. Boyd, L. E. Ghaoui, E. Feron, V. Balakrishnan, *Linear Matrix Inequalities in System and Control Theory*, Philadelphia , Pennsylvania: SIAM, 1994.

[50] H. Kwakernaak, "Robust control and H∞-optimization—Tutorial paper," A*utomatica*, vol. 29, no. 2, pp. 255-273, March 1993.

[51] J. Lofberg, "YALMIP: a toolbox for modeling and optimization in MATLAB," *IEEE International Symposium on Computer Aided Control Systems Design*, pp.284-289, 2-4 Sept. 2004, Taiwan.

[52] S. Seshagiri and H. K. Khalil, " On Introducing Integral Action in Sliding Mode Control", in *Proc. of 41st IEEE Conference on Decision and Control*, pp.1473-1476, 10-13 December 2002.

[53] C. Edwards and S. K. Spurgeon, *Sliding Mode Control: Theory and Applications*, Abingdon, UK: Taylor and Francis, 1998.

[54] B. Drazenovic, "The Invariance condition in variable structure systems", *Automatica*, vol.5, no. 3, pp.287-295, 1969.

[55] D. Karnopp, "Computer Simulation of Stick-Slip Friction in Mechanical Dynamic Systems", *Journal of Dynamical Systems , Measurement and Control, Transactions of the ASME*, vol.107, March 1985, pp. 100-103

[56] S. A. Campbell, S. Crawford and K. Morris, "Friction and The Inverted Pendulum Stabilization Problem", *Journal of Dynamical Systems , Measurement and Control, Transactions of the ASME*, vol. 130, no. 5, 2008, 0545021-0545027.

[57] Frédéric Moisy, University of Paris-Sud, Ezyfit: A curve fitting toolbox for MATLAB, Paris: France, Available Online: http://www.fast.u-psud.fr/ezyfit/

[58] B.D. Anderson and J.B. Moore, "Optimal Control Systems", *Prentice Hall Inc.*, N.J: USA, 1971.

[59] D.S. Naidu, "Optimal Control Systems", *CRC Press*, 2006.

Thesis Dissemination

Journals

[1] A. Ghosh, T. R. Krishnan, B. Subudhi, "Robust PID Compensation of an Inverted Cart-Pendulum System: An Experimental Study", *IET Control Theory and Applications*, doi: 10.1049/iet-cta.2011.0251

Conference

[1] T.R. Krishnan, S. S. Ghosh, A. Ghosh, B. Subudhi, "Periodic Compensation of an Inverted-Cart Pendulum System", Advances in Control and Optimization of Dynamical Systems (ACODS) , IISC Bangalore, Feb 16-18 2012.